



Universidade do Minho
Escola de Ciências

Joana Raquel da Silva Martins

The role of CXCR4 in cancer exosomes and metastasis

Dissertação de Mestrado

Mestrado em Genética Molecular

Trabalho efetuado sob a orientação de

Prof.^a Doutora Sónia Maria Almeida Guedes de Melo

Co-orientação: Doutora Ana Arminda Lopes Preto de
Almeida

Novembro de 2018

Declaração

Nome: Joana Raquel da Silva Martins

Endereço eletrónico: joana_jrsm@hotmail.com

Telefone: 935719662

Número de Bilhete de Identidade: 14528274

Título da tese de mestrado: “The role of CXCR4 in cancer exosomes and metastasis”

Orientador: Professora Doutora Sónia Maria Almeida Guedes De Melo

Coorientador: Professora Doutora Ana Arminda Lopes Preto de Almeida

Ano de conclusão: 2018

Designação do Mestrado: Mestrado em Genética Molecular

DE ACORDO COM A LEGISLAÇÃO EM VIGOR, NÃO É PERMITIDA A REPRODUÇÃO DE
QUALQUER PARTE DESTA TESE/TRABALHO.

Universidade do Minho, 30 de novembro de 2018

Assinatura: Joana Raquel Silva Martins

ACKNOWLEDGMENTS

The conclusion of my master's degree marks the end of another important step in my academic career and personal life. During this last year, I lived a mixture of emotions, with moments of pure happiness and others with frustration and hopelessness. I could not have made it this far if I had not been surrounded by incredible people who gave me love, hope and reminded me every day of my capabilities.

First, I would like to thank my supervisor, Sónia Melo, for having welcomed me into his team with open arms. Thank you for showing me that without effort and dedication we cannot achieve our goals and that we need to give our best in everything we do. Thank you for all the scientific knowledge and personal advice, it was a great pleasure to work with you.

To the Melo team, Nuno, Carolina, Bárbara, Inês, Patty and Soraia, thank you all for helping me without hesitation when I needed. A special thank you to Nuno for being my mentor and helping in everything I asked for. Thanks to Carolina for all the scientific and mostly non-scientific advice and for taking care of me every time I was sick. Thank you Inês for the good advices and thank you, Patty, for all the good moments, courage for your master's thesis you will rock it.

Thank you to the Gedy TEAM for all the good moments we been through it was a pleasure be part of this incredible group. May the force be with you!

To my girls, Rosa, Adriana, Mafalda, Joana P, Ana Maria e Mónica thank you for the long talks about the future, the silly advices and all the funny moments we have been through together.

A big thank you to my boyfriend for being my best friend, for all the love, for the unconditional support and for always believing in me.

A special thank you to my brother for making my world a wonderful place even when he is annoying. I would do anything for you.

And finally, a big thank you to my parents for all the efforts they made to give me this incredible opportunity and for believing in me even when I doubted of my abilities. I love you!

Thank you all from the bottom of my heart!

This work was developed at Sonia Melo team at Ipatimup/Instituto de Investigação e Inovação em Saúde (i3S), University of Porto.

Sonia Melo team is supported by the project NORTE-01-0145-FEDER-000029, Norte Portugal Regional Programme (NORTE 2020), under the PORTUGAL 2020 Partnership Agreement, through the European Regional Development Fund (ERDF) and national funds through FCT - Foundation for Science and Technology IF/00543/2013/CP1184/CT0004, PTDC/BIM-ONC/2754/2014, POCI-01-0145-FEDER-32189 and Astrazeneca Foundation, FAZ Ciencia Award.



THE ROLE OF CXCR4 IN CANCER EXOSOMES AND METASTASIS

ABSTRACT

Exosomes are central mediators of intercellular communication. Exosomes are extracellular vesicles that carry proteins, RNA and DNA of the cells of origin, transfer their cargo to other cells and have the potential to re-educate recipient cells. Cancer exosomes have been involved in almost all steps during tumor progression up to metastasis and therapy resistance. However, the mechanisms underlying the involvement of cancer exosomes in the metastatic process are not fully understood. The chemokine receptor CXCR4 and its ligand CXCL12 represent one of the most studied chemokine axis in metastasis. CXCL12 is highly expressed in tissues like lungs, liver, and bone marrow. CXCR4/CXCL12 interaction results in increased proliferative, migratory, and invasive properties of tumor cells. Although expression patterns vary among cancer types, CXCR4 has been implicated in nearly every major malignancy and plays a prominent role in pancreatic cancer development and progression. Our work is based on the hypothesis that CXCR4⁺ pancreatic cancer exosomes are preferentially retained at CXCL12-enriched organs. In the present work, we establish the PANC-1 CXCR4-EYFP clone and developed a PANC-1 CXCR4-EYFP orthotopic mouse model to study the *in vivo* retention of CXCR4⁺ exosomes at CXCL12 enriched sites. CXCR4-EYFP orthotopic tumors secrete CXCR4⁺ exosomes that are found in circulation. We demonstrate for the first time that pancreatic cancer exosomes have a selective loading of CXCR4 receptor at their surface, along with the CD133 cancer-stem cell marker. Moreover, we show that CXCR4⁺ exosomes show a higher retention in plugs containing recombinant CXCL12 when compared with control plugs. Our results suggest that the selective loading of CXCR4 at exosomes surface could contribute for a differential distribution of cancer exosomes *in vivo*. This study provides new insights into the emerging role of exosomes in cancer, more specifically it addresses the biological relevance of CXCR4 in pancreatic cancer progression and metastasis.

Keywords: Pancreatic cancer, Exosomes, CXCR4, CXCL12, Metastasis, Pre-metastatic niche

O PAPEL DO CXCR4 EM EXOSSOMAS TUMORAIS E EM METÁSTASES

RESUMO

Exossomas são mediadores importantes na comunicação intracelular. Exossomas são vesículas extracelulares que transportam proteínas, moléculas de RNA e DNA que podem ser transferidas para outras células, tendo o poder de as alterar. Os exossomas tumorais estão envolvidos em quase todas as etapas da progressão tumoral, incluindo metástases e resistência à terapia. No entanto, o mecanismo subjacente ao papel dos exossomas tumorais no processo metastático não é totalmente compreendido. O recetor de quimiocinas CXCR4 e o seu ligando CXCL12 representam um dos eixos de quimiocinas mais estudados neste processo. O CXCL12 é muito expresso em tecidos como pulmão, fígado e medula óssea. A interação CXCR4/CXCL12 resulta num aumento das propriedades proliferativas, migratórias e invasivas das células tumorais. Embora os padrões de expressão variem entre os diferentes tipos de cancro, o CXCR4 tem vindo a ser implicado em quase todos os tipos de cancro e desempenha um papel proeminente no desenvolvimento e progressão do cancro do pâncreas. O nosso trabalho tem como base a hipótese de que os exossomas contendo CXCR4 provenientes de células tumorais pancreáticas são preferencialmente retidos em órgãos enriquecidos em CXCL12. Neste trabalho, desenvolvemos um modelo ortotópico de cancro pancreático usando a linha celular PANC-1 CXCR4-EYFP. Este modelo permitiu estudar a retenção *in vivo* de exossomas CXCR4⁺ em locais enriquecidos em CXCL12. Tumores ortotópicos CXCR4-EYFP produzem exossomas CXCR4-EYFP, encontrados em circulação. Demonstramos pela primeira vez que o recetor CXCR4, juntamente com CD133, são seletivamente acumulados na superfície de exossomas de cancro de pâncreas. Além disso, mostramos que os exossomas CXCR4⁺ mostram maior retenção em plugs contendo a proteína recombinante CXCL12 quando comparado com plugs controlo. Estes resultados sugerem que a acumulação seletiva de CXCR4 na superfície de exossomas tumorais poderá contribuir para a sua distribuição diferencial *in vivo*. Este estudo fornece novas informações sobre o papel emergente de exossomas no processo tumoral, abordando a relevância biológica do CXCR4 na progressão do cancro do pâncreas e no estabelecimento de metástases.

Palavras-chave: Cancro pancreático, Exossomas, CXCR4, CXCL12, Metástases, Nicho pré-metastático

TABLE OF CONTENTS

ACKNOWLEDGMENTS.....	iii
ABSTRACT	v
RESUMO.....	vii
TABLE OF CONTENTS.....	ix
GLOSSARY OF ABBREVIATIONS AND ACRONYMS	xi
LIST OF FIGURES	xii
1. INTRODUCTION	1
1.1. Cancer	2
1.2. Pancreatic Cancer	3
1.2.1. The KPC model	4
1.3. Chemokines in cancer	5
1.3.1. CXCR4 – CXCL12 axis	6
1.3.2. CXCR4-CXCL12 axis in PDAC.....	8
1.4. Exosomes.....	10
1.4.1. Exosomes biogenesis	12
1.4.2. The composition of tumor-derived exosomes	14
1.4.3. Exosomes in PDAC metastasis	17
1.5. Rationale	19
1.6. Work plan and aims	20
2. MATERIAL AND METHODS.....	21
2.1. Cell culture	22
2.2. pEYFPCXCR4-N1 plasmid expansion.....	22
2.3. Cell line transfection	22
2.4. Exosomes isolation.....	23
2.4.1. Cell culture media.....	23
2.4.2. Serum.....	23
2.5. Flow cytometry analysis in cells	23
2.5.1. Cells	23
2.5.1.1. Membrane.....	24
2.5.1.2. Intracellular	24

2.5.2.	Exosomes	24
2.5.2.1.	Exosomes from cell culture medium	24
2.5.2.2.	Exosomes from serum samples.....	25
2.6.	Protein extraction and quantification	25
2.7.	Western blot	26
2.8.	<i>In vitro</i> co-culture	26
2.9.	KPC mice euthanasia	27
2.10.	H&E stain	27
2.11.	Immunohistochemistry (IHC)	27
2.12.	Orthotopic injection of PANC-1 CXCR4-EYFP cells.....	29
2.13.	Matrigel Plugs <i>in vivo</i> experiment.....	29
2.14.	Procedure for mice euthanasia	30
2.15.	Imaging acquisition and processing.....	31
2.16.	Statistical analysis	31
3.	RESULTS	33
3.1.	CXCR4 is expressed in PDAC cell lines and co-express with CD133.....	34
3.2.	Exosomes of PDAC cell lines are CXCR4 and CD133 positive	35
3.3.	Establishment of CXCR4-EYFP PDAC cell lines.....	37
3.4.	CXCR4-EYFP PDAC cell lines secrete CXCR4-EYFP+ exosomes	39
3.5.	CXCR4-EYFP exosomes flow between cancer cells	41
3.6.	PANC-1 CXCR4-EYFP+ exosomes accumulate more in CXCL12-embedded plugs	41
3.7.	CXCR4+ exosomes are not enriched in the serum of KPC mice with higher frequency of metastasis.....	46
4.	DISCUSSION.....	50
5.	CONCLUSION AND.....	59
	FUTURE PERSPECTIVES	59
	REFERENCES.....	61

GLOSSARY OF ABBREVIATIONS AND ACRONYMS

7TM - seven transmembrane domain receptors

Asn - Asparagine

bFGF - Basic fibroblast growth factor

BMDCs - bone marrow-derived cells

CD133 - prominin-1

CDKN2A - cyclin-dependent kinase Inhibitor 2A

CSC - cancer stem cells

CTCs - circulating tumor cells

CXCL12 - C-X-C motif chemokine 12

CXCR4 - C-X-C chemokine receptor type 4

DTCs - Disseminated Tumor Cells

ECM - extracellular matrix

ESCRT - endosomal sorting complex required for transport

EVs - extracellular vesicles

FasL - Fas ligand

FN - fibronectin

GC - Golgi complex

GEMM - genetically engineered mouse model

GPC1 - glypican-1

GPCRs - G protein-coupled receptors

HER2/neu - Human Epidermal growth factor Receptor 2

HIF-1 - Hypoxia-inducible factors

IFN- γ - Interferon gamma

IL-1 β - Interleukin 1 beta

ILVs - intraluminal vesicles

KPC - Kras^{LSL.G12D/+}; p53^{R172H/+}; PdxCretg/+ model

KRAS - Kristen rat sarcoma viral oncogene

Lys - Lysine

MET - tyrosine-protein kinase Met

MIF - migration inhibitory factor

MVB - multivesicular body

NF- κ B - factor nuclear kappa B

PC - pancreatic cancer

PDAC - Pancreatic Ductal Adenocarcinoma

PD-L1 - Programmed death-ligand 1

PGE2 - prostaglandin E2

RER - rough endoplasmic reticulum

SDF-1 - Stromal cell-derived factor 1

Ser - Serine

SMAD4 - Mothers against decapentaplegic homolog 4

TAA - tumor associated antigens

TGF- β 1 - Transforming growth factor beta

TME - tumor microenvironment

TNF- α - Tumor necrosis factor

TP53 - Tumor promoting p53 gene

VEGF - Vascular endothelial growth factor

VEGFR1 - vascular endothelial growth factor receptor 1

LIST OF FIGURES

FIGURE 1. THE HALLMARKS OF CANCER	3
FIGURE 2. EXOSOME BIOGENESIS AND SECRETION	13
FIGURE 3. SCHEMATIC REPRESENTATION OF THE FAMILIES OF PROTEINS, NUCLEIC ACIDS AND LIPIDS PRESENT IN EXOSOMES	16
FIGURE 4. CXCR4 IS EXPRESSED IN PDAC CELL LINES AND CO-EXPRESSES WITH CD133... 35	
FIGURE 5. EXOSOMES OF PDAC CELL LINES ARE CXCR4 AND CD133 POSITIVE.	36
FIGURE 6. ESTABLISHMENT OF CXCR4-EYFP PDAC CELL LINES.....	38
FIGURE 7. CXCR4-EYFP PDAC CELL LINES SECRETE CXCR4-EYFP+ EXOSOMES	40
FIGURE 8. CXCR4-EYFP EXOSOMES FLOW BETWEEN CANCER CELLS.....	42
FIGURE 9. PANC-1 CXCR4-EYFP ⁻ EXOSOMES ACCUMULATE MORE IN CXCL12-EMBEDDED PLUGS.....	45
FIGURE 10. CXCR4-EYFP ⁻ EXOSOMES ARE PRESENT IN THE BLOODSTREAM.....	47
FIGURE 11. CXCR4 ⁺ EXOSOMES ARE NOT ENRICHED IN THE SERUM OF KPC MICE WITH HIGHER FREQUENCY OF METASTASIS.	49

1.INTRODUCTION

1.1. Cancer

Cancer is one of the main causes of mortality with over 8.8 million deaths in 2015 (“Cancer,” 2017). Early detection and a correct cancer diagnosis are essential for adequate and effective treatment, however, most cancers are diagnosed at very advanced stages (Crowell, Ransohoff, & Kramer, 2010). The risk of developing cancer depends on several factors, including age, genetics, and exposure to risk factors (smoking, insufficient physical activity, alcohol, diet, overweight and obesity, and infections) (White et al., 2014). During the past decades, cancer research has revealed an extensive insight into the multitude of cellular processes involved in malignant transformation (D Hanahan & Weinberg, 2000). However, more research is needed to better understand this complex and heterogeneous disease and help find and develop more effective treatments.

Carcinogenesis is a multistep process in which genetic and epigenetic alterations drive the progressive transformation of normal cells into malignant cells (Pietras & Östman, 2010). In 2000, Hanahan and Weinberg enumerated six hallmarks of cancer that offers a logical framework for understanding the variety of neoplastic diseases (D Hanahan & Weinberg, 2000). The progressive change of normal cells to neoplastic cells is associated with the acquisition of these different hallmarks (Douglas Hanahan & Weinberg, 2011). These capabilities might be acquired in different orders, depending on the type and subtype of cancer (D Hanahan & Weinberg, 2000). The alterations that lead to tumor initiation and progression are: self-sufficiency in growth signals, insensitivity to anti-growth signals, evading apoptosis, limitless replicative potential, sustained angiogenesis and tissue invasion and metastasis (D Hanahan & Weinberg, 2000). However, the progress in cancer research revealed that to understand the biology of tumors is not enough to look to cancer cells individually but instead we need to incorporate the contributions of the microenvironment to tumor progression (Pietras & Östman, 2010). New hallmarks emerged: genome instability and mutations, tumor-promoting inflammation, the reprogramming of energy metabolism and evading immune destruction (Douglas Hanahan & Weinberg, 2011). The establishment of these hallmarks (**Figure 1**) provided a useful conceptual framework for understanding the complex biology of cancer and led to the development of new therapeutic approaches (Douglas Hanahan & Weinberg, 2011).

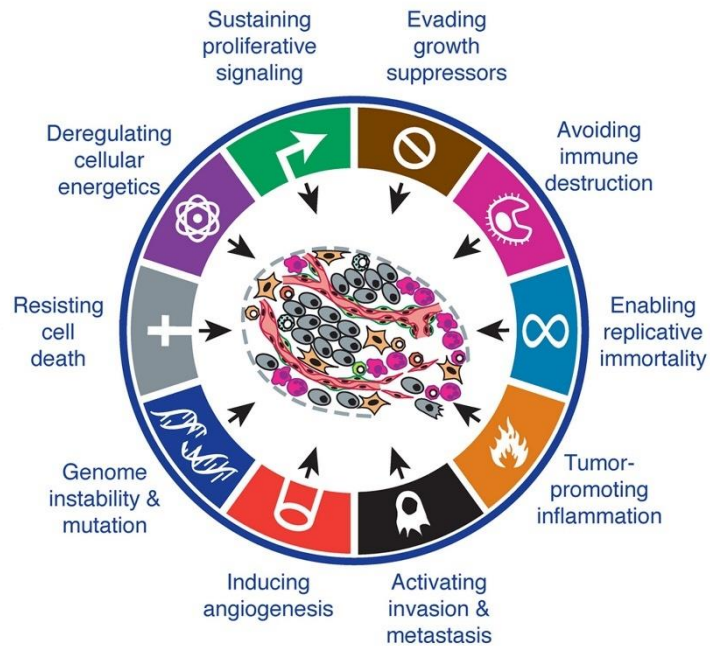


Figure 1. The Hallmarks of Cancer. Illustration highlighting the main biological and cellular processes involved in tumor initiation and progression. Adapted from Douglas Hanahan and Weinberg (2011)

1.2. Pancreatic Cancer

Pancreatic cancer (PC) is currently one of the major causes of cancer-associated mortality and is predicted to be the second leading cause of cancer-related mortality within the next decade (Kleeff et al., 2016). Pancreatic cancer is an aggressive disease that harbours multiple genetic and epigenetic alterations and has complex and dense tumor microenvironments. Characterized for being resistant to most conventional treatment options, this disease is associated with an extremely poor prognosis because is usually diagnosed at advanced stages due to nonspecific symptoms (Kleeff et al., 2016). Around 80–90% of PC patients present with either locally advanced or metastatic disease (Bilimoria et al., 2007). Surgery offers the only potentially curative treatment, however only 15–20 % of patients have localized, non-metastatic disease suitable for resection. After the surgical intervention, most patients develop disease recurrence within a year (Labori et al., 2016). Despite continuous research efforts, the incidence of PC is rising and the overall prognosis of PC patients remains extremely poor (Siegel, Ma, Zou, & Jemal, 2014).

In pancreatic cancer it has been described a multitude of histologically distinct precursor lesions. PC most frequently arises from pancreatic intraepithelial neoplasia (PanIN), the classic

pre-neoplastic lesions, however, PC can also arise from larger precursor lesions (namely, intraductal papillary mucinous neoplasms (IPMNs) and mucinous cystic neoplasms) (Hezel, Kimmelman, Stanger, Bardeesy, & Depinho, 2006) (Tanaka, 2014) The majority of pancreatic cancers are adenocarcinomas, and pancreatic ductal adenocarcinoma (PDAC) comprises 90% of all PC cases (Biankin et al., 2012). The molecular pathology of pancreatic cancer is dominated by activating mutations in KRAS, which are present in >90% of tumors. KRAS is an oncogene that mediates a range of cellular functions, including proliferation, cell survival, cytoskeletal remodelling, and motility, among others. Moreover, inactivating mutations in tumor suppressor genes such as TP53, CDKN2A and SMAD4 occur in 50–80% of pancreatic cancers, while other genes (ARID1A, MLL3 and TGFBR2) are mutated in ~10% of cases (D. K. Chang, Grimmond, & Biankin, 2014). The microenvironment of pancreatic cancer is characterised by a profound fibrous inflammatory reaction termed desmoplasia that results in a hypoxic environment for cancer cells (Westphalen & Olive, 2012a). This desmoplastic reaction is a direct consequence of immune cell infiltration and subsequent inflammation (Feig et al., 2012). The atypical tumor microenvironment (TME) found within these tumors can comprise up to 90% of the mass. This desmoplastic reaction plays a role in tumor development, progression, and chemotherapeutic resistance (Neesse et al., 2011). PDAC is one of the most stroma-rich cancers. The composition of the stroma can include cellular and acellular components, such as fibroblasts, myofibroblasts, pancreatic stellate cells, immune cells, blood vessels, extracellular matrix and soluble proteins such as cytokines and growth factors (Feig et al., 2012).

1.2.1. The KPC model

In a way to improve the knowledge about this disease, model systems of pancreatic cancer have been developed, to complement the traditional cell line and xenograft models and include genetically engineered mouse model (GEMM) and organoid cultures (Kleeff et al., 2016). Mouse models of pancreatic cancer that somatically target mutant alleles to the mouse pancreas have demonstrated that oncogenic KRAS is uniquely sufficient to initiate PanIN that spontaneously progress to locally invasive and metastatic pancreatic cancer (Hingorani et al., 2003). Different genetic and chemical approaches to generate pancreatic cancer in mice were made. However, it was the generation of the K-ras^{LSL.G12D} mouse that allowed tissue-specific expression of mutant K-ras^{G12D} and thereby activation of the Ras pathway. The combination of oncogenic KRAS, with additional mutations in the canonical tumor suppressor genes CDKN2A (encoding p16), TP53 or SMAD4 have been shown to accelerate pancreatic tumor progression (Hruban et al., 2006). These

mutations are targeted specifically to the mouse pancreas using Cre-Lox technology (Hingorani et al., 2005). The KPC mice (K-ras^{LSL.G12D/+}; p53^{R172H/+}; PdxCre) display disease progression that closely resembles human disease. The mice are born with a histologically normal pancreas, however, by 8 to 10 weeks of age, KPC mice harbor precursor lesions, or pancreatic intraepithelial neoplasia (PanIN). By 16 weeks of age, most KPC mice have developed locally invasive PDAC that is accompanied by a dense desmoplastic reaction. At this time point, most mice show evidence of tumor development and biliary obstruction. With disease progression, mice can also develop co-morbidities associated with human PDAC such as cachexia, jaundice, weight loss, and malignant ascites due to the peritoneal spread of disease. Metastasis are observed in 80% of KPC mice located at the same sites most commonly observed in human PDAC patients (liver, lung, and peritoneum) (Hingorani et al., 2005). Ultimately, these animals die of PDAC with a median survival of 5.5 months. The tumors from KPC mice generally present the most common morphology observed in humans with moderately differentiated ductal morphology with extensive stromal desmoplasia (Westphalen & Olive, 2012a). These tumors have many of the immunohistochemical markers associated with human disease, harbor complex genomic rearrangements indicative of genomic instability and are predominantly resistant to chemotherapy (Hingorani et al., 2005).

1.3. Chemokines in cancer

The poor prognosis associated with pancreatic cancer is largely attributed to the fact that, by the time it is diagnosed the patient already has metastasis. The knowledge about the signalling events that mediate the progression from pancreatic cancer precursors to invasive, metastatic tumors is extremely limited (Sohn & Yeo, 2000). The efforts to understand these mechanisms have shown that chemokines and their respective receptors are directly involved in the molecular control of cancer metastasis and organ-specific homing of circulating cancer cells (Seema Singh, Sadanandam, & Singh, 2007). The expression of chemokine receptors in cancer cells is not random and the chemokine receptor CXCR4 appears to be the most common chemokine receptor expressed in most types of cancer cells (Zlotnik, 2006). Several studies suggest that the interaction of CXC motif chemokine receptor (CXCR) 4 with CXCL12 appears to have an important role in tumor proliferation, invasion, angiogenesis, metastasis and migration in numerous types of cancer (Burger & Kipps, 2006; Sun et al., 2010; Vandercappellen, Van Damme, & Struyf, 2008).

1.3.1. CXCR4 – CXCL12 axis

Chemokines are low molecular weight signalling proteins (8-10 kDa), characterized by a cysteine motif. They can be classified into four groups (CXC, CC, C and CX3C) depending on the position of the first two cysteines (Zlotnik & Yoshie, 2000). Chemokines interact with chemokine receptors activating downstream signalling pathways. The chemokine receptors are members of the seven transmembrane domain (7TM) G protein-coupled receptor superfamily (GPCRs) that mediate chemotactic activity in leukocytes but are expressed on a wide range of cell types (Murphy, 1994) (Premack & Schall, 1996). Beyond their central role in development and inflammation, chemokines are implicated in a broad range of human diseases, including autoimmune and inflammatory diseases and cancer (Balkwill, 2004a) (Charo & Ransohoff, 2006).

The CXCR4 is one of the best-studied chemokine receptors, primarily due to its role as a co-receptor for HIV entry as well as its ability to mediate the metastasis of a variety of cancers (Busillo & Benovic, 2007). CXCR4 is by far the most common chemokine receptor expressed in cancer cells and its expression has been detected in 23 different cancers including kidney, lung, brain, prostate, breast, pancreas, ovarian, and melanomas (Balkwill, 2004b). The chemokine receptor CXCR4 selectively binds the CXC chemokine Stromal Cell-Derived Factor 1 (SDF-1) also known as CXCL12 (Murphy et al., 2000).

The basal transcription of CXCR4 is mainly controlled by the opposing actions of two transcriptional regulators, however, a number of signalling molecules have been shown to affect its transcription (Busillo & Benovic, 2007). For example, the presence of intracellular second messengers, such as calcium and cyclic AMP can increase the CXCR4 expression (Moriuchi, Moriuchi, Turner, & Fauci, 1997). Also, several cytokines (IL-2, IL-4, IL-7, IL-10, IL-15, TGF-1 β) and growth factors such as basic fibroblast growth factor (bFGF) can also increase the expression of CXCR4 (Moriuchi et al., 1997) (Jourdan et al., 2000). On the other hand, inflammatory cytokines such as tumor necrosis factor- α (TNF- α), interferon- γ (INF- γ), and IL-1 β have all been shown to attenuate CXCR4 expression (Gupta, Lysko, Pillarisetti, Ohlstein, & Stadel, 1998). During cancer progression, there are several mechanisms that can enhance CXCR4 expression. The hypoxic environment induces the activation of hypoxia-inducible factor 1 (HIF-1) that subsequently promotes the expression of several target genes, including CXCR4.

There are several mechanisms that can enhance CXCR4 expression during cancer progression. For instance, hypoxia induces the activation of hypoxia-inducible factor 1 (HIF-1) which

in turn promotes expression of several target genes, including CXCR4. Also, vascular endothelial growth factor (VEGF) or activation of nuclear factor kappa B (NF- κ B) enhances CXCR4 expression in breast cancer-promoting invasion and metastasis, respectively (Busillo & Benovic, 2007). Regarding the protein expression, there is a number of co-translational modifications that contribute to the expression and function of CXCR4 (Busillo & Benovic, 2007). CXCR4 exhibits significant heterogeneity in cells, which may be a result of ubiquitination, differential glycosylation or the formation of oligomers (Lapham et al., 2002). Glycosylation of CXCR4 is important for CXCL12 binding and within the extracellular domain of CXCR4, there are two potential N-linked glycosylation sites (Asn11 and Asn176). Both sites undergo glycosylation when CXCR4 is expressed, however, only Asn11 appears to be glycosylated in mammalian cells. (Busillo & Benovic, 2007).

The interaction between CXCR4 and CXCL12 has been proposed to occur through a two-step process. The initial interaction is believed to result in a conformational change in the receptor that then facilitated the final interaction. This process requires the integrity of both CXCL12 and CXCR4 (Crump et al., 1997). Upon SDF binding to CXCR4, several signalling pathways are activated leading to different biological responses. Once the pathways activated can be either G protein-dependent or G Protein Independent, the outcomes caused by CXCR4 activation may differ between CXCR4⁺ cell types (Busillo & Benovic, 2007).

Upon CXCR4 activation, the receptor is phosphorylated and internalized (Haribabu et al., 1997). It has been described that membrane CXCR4 undergoes an internalization process through a clathrin-mediated endocytic pathway (Signoret et al., 1997) (Zhang et al., 2004). After internalization, CXCR4 can be recycled back to the plasma membrane but usually, it is ubiquitinated and sorted to the lysosome for further degradation (Orsini, Parent, Mundell, & Benovic, 1999) (Marchese, Chen, Kim, & Benovic, 2003). It has been found that breast cancer cells that are HER2/neu positive have increased expression of CXCR4 as a result of the inhibition of receptor ubiquitination (Y. M. Li et al., 2004). Studies have shown that CXCR4 is most likely ubiquitinated on one of three lysines residues (Lys327, Lys331, or Lys333) in the C-terminal tail. Mutation of these three residues to arginine eliminates ubiquitination and degradation of the receptor (Marchese & Benovic, 2001). Mutation of Ser330 to alanine partially inhibits CXCR4 degradation without affecting receptor internalization while mutation of Ser324 and Ser325 partially inhibited SDF-promoted internalization but completely disrupted degradation (Marchese & Benovic,

2001). These results suggest that the fate of the receptor after internalization may be dictated by modifications that occur on specific residues (Busillo & Benovic, 2007).

1.3.2. CXCR4-CXCL12 axis in PDAC

In pancreatic cancer, the CXCR4/CXCL12 axis has been implicated in almost every aspect of tumorigenesis, especially in the invasive and metastatic process (Sleightholm et al., 2017). Patients with high CXCR4-expressing tumors had a worse outcome than those with low CXCR4 expression (Maréchal et al., 2009). Moreover, this chemokine axis is also altered in response to chemotherapy. Gemcitabine that remains the first-line chemotherapeutic agent used for PDAC, was shown to upregulate CXCR4 expression in PDAC cells in a dose- and time-dependent manner inducing chemoresistance (Arora et al., 2013). In another study, CXCL12 was shown to activate a series of signalling events in pancreatic cancer cells and counteracts the cytotoxic effects of gemcitabine (S Singh, Srivastava, Bhardwaj, Owen, & Singh, 2010).

CXCR4 is expressed in several pancreatic cancer cell lines, however, its expression is higher in cell lines originated from metastatic or ascitic lesions, compared with cell lines derived from primary tumors (Marchesi et al., 2004). Interestingly, it was described the expression of CXCR4 in a subpopulation of pancreatic cancer stem cells (Hermann et al., 2007). Several studies have been providing multiple lines of evidence for the role of CSCs in pancreatic tumor growth, tumor metastasis, and drug resistance (Castellanos, Merchant, & Nagathihalli, 2013; Hermann et al., 2007; Xia et al., 2012). Cancer stem cells (CSCs), also known as cancer-initiating cells, represent a biologically distinct population of cells within the tumor. They are capable of self-renewal and differentiation into any type of cell found in the tumor, allowing the maintenance of the tumor (Hermann et al., 2007). CD133, a pentaspan membrane glycoprotein, has been used as a stem cell biomarker for the identification of a subpopulation of stem-like cells (Z. Li, 2013). Hermann et al. showed that pancreatic CSCs do not represent a homogeneous population of tumor-initiating cells (Hermann et al., 2007). They identified a subpopulation of migrating CSCs critically involved in tumor metastasis that is characterized by CD133+CXCR4+ expression. The migration of this invasive CSCs is primarily mediated through activation of the CXCR4 receptor. This subpopulation can be detected in the invasive front in the pancreas as well as in the circulating blood. Although CD133+ cells were able to produce tumors, CXCR4 co-expression was essential for producing metastasis. Elimination of these migrating CSC (CD133+ CXCR4+) virtually abrogated the metastatic activity of pancreatic cancer cells. (Hermann et al., 2007). Moreover, the inhibition of

the CXCR4 receptor by AMD3100, a specific antagonist of CXCR4, prevented the metastatic behaviour of these cells (Hermann et al., 2007).

Emerging evidence suggests that CXCR4/CXCL12 axis facilitate the spread of migrating tumor cells expressing CXCR4 towards gradients of CXCL12 and homing to specific organs (Balic, Dorado, Alonso-Gómez, & Heeschen, 2012; Marchesi et al., 2004; Sleightholm et al., 2017). As mentioned before, CXCL12, the specific ligand for CXCR4, is strongly expressed in lung, liver, bone marrow, and lymph nodes that represent the most common sites of metastasis in pancreatic cancer (S Singh et al., 2010). This suggests a mechanism analogue to the directed homing of leukocytes where these gradients of CXCL12, provide chemotactic, survival, and proliferative signals that guide implantation and support growth in these tissues (Sleightholm et al., 2017). Moreover, the chemotaxis in CXCR4-positive pancreatic cancer cell lines induced by the chemokine CXCL12 was inhibited by two different CXCR4 antagonists (AMD3100 and TN14003) (Marchesi et al., 2004; Mori et al., 2004). Together, this data provides a strong evidence for the crucial role of the CXCR4/CXCL12 axis in metastasis (Balic et al., 2012).

Nevertheless, tumor progression towards metastasis is a complex multi-step process in which only a small percentage of tumor cells that are released from a primary tumor successfully form distant lesions (Luzzi et al., 1998). Besides the intrinsic properties of circulating cancer cells, the local microenvironment at the metastatic organ is critical in determining their fate (Sleeman, 2012). The idea that a nutritive microenvironment is required for the survival and outgrowth of disseminating tumor cells (DTCs) at the secondary sites led to the conception of the term: metastatic niche (Psaila & Lyden, 2009; Sleeman, 2012). Steven Paget's "Seed and Soil" hypothesis was the first study introducing the concept that metastasis is dependent on the interactions between 'seeds' (or the cancer cells) and the 'soil' (or the host microenvironment). The hypothesis sets that just as certain plants and life forms succeed exclusively in distinct ecosystems that are favourable to their survival, a receptive microenvironment is required for malignant cells to engraft distant tissues and form metastasis (Paget, 1889). Fidler *et al.* demonstrated that cancer cells derived from a certain metastatic site displayed enhanced abilities to metastasize to that specific organ, providing support for Paget's organ-specific metastasis theory (Hart2 & Fidler, 1980). Additional fundamental discoveries revealed that tumors induce the formation of microenvironments in distant organs that are beneficial to the survival and outgrowth of tumor cells before their arrival at these sites (Peinado et al., 2017).

The organ specificity observed during the metastatic process is known as organotropism and remains one of the most intriguing unanswered questions in cancer research (Peinado et al., 2017). Furthermore, recent discoveries suggest that microenvironment changes in organs before the arrival of DTCs can be induced by factors secreted systemically by primary tumors, leading to the formation of pre-metastatic niches (Sleeman, 2012). This led to the concept of the pre-metastatic niche in which, a sequence of events prepares the future metastatic sites for the arrival of CTCs, supporting the engraftment and survival of these incoming metastatic cells (Kaplan et al., 2005; Peinado, Lavotshkin, & Lyden, 2011; Sceneay, Smyth, & Möller, 2013). This suggests that the occurrence of metastasis in specific organs is not random, but a pre-determined event, in which cancer cells leave a primary tumor already with a defined destination (Peinado et al., 2011).

Early studies regarding the pre-metastatic niche described that haematopoietic cells derived from the bone marrow that express vascular endothelial growth factor receptor 1 (VEGFR1) and the fibronectin receptor $\alpha4\beta1$ (also known as integrin $\alpha4\beta1$) localize at pre-metastatic sites prior to the arrival of tumor cells, and are key components of the pre-metastatic niche (Kaplan et al., 2005). At the pre-metastatic organs, the bone marrow-derived cells (BMDCs) help to create a suitable niche by altering the microenvironment through processes that include extracellular matrix (ECM) remodelling, immunosuppression, inflammation, and vascular hyperpermeability (Sceneay et al., 2013). Several reports revealed that a primary tumor promotes mobilization and recruitment of these cells to future metastatic sites through secretion of a variety of factors (Kaplan, Rafii, & Lyden, 2006). These tumor-secreted factors were shown to influence the metastatic process by inducing vascular leakiness (Zhou et al., 2014), promoting the recruitment of pro-angiogenic immune cells (Q. Chang et al., 2013), and influencing organotropism (Lu & Kang, 2007). Since they actively influence cell behaviour, the tumor-secreted soluble factors are recognized as a mechanism of cell-to-cell communication within the tumor microenvironment, as well as the generation of suitable niches in distant organs (Peinado et al., 2011). Recently, it was demonstrated that exosomes are one of the tumor-derived factors inducing vascular leakiness, inflammation, and recruitment of BMDCs during pre-metastatic niche formation and metastasis (Peinado et al., 2012).

1.4. Exosomes

Cell communication is crucial to maintain correct coordination among different cell types within tissues (Camussi, Deregibus, Bruno, Cantaluppi, & Biancone, 2010). Cells may communicate and

exchange information through different mechanisms. This communication may involve a direct cell-to-cell contact or gradients formed by soluble (paracrine) mediators, which may also circulate in blood and body fluids and act in a regional or systemic (endocrine) manner. This information is then translated into activation of intracellular signalling networks and changes the behaviour of individual cells and their populations (Lee, Asti, & Magnus, 2011). Recently, the secretion of extracellular vesicles (EVs) was proposed as a new mechanism of cell communication, providing another dimension of cellular crosstalk (Ratajczak, Wysoczynski, Hayek, Janowska-Wieczorek, & Ratajczak, 2006) (Zappulli, Friis, Fitzpatrick, Maguire, & Breakefield, 2016). For a long time, the secretion of EVs was believed to be a way of eliminating unnecessary compounds from the cell. (Johnstone, Adam, Hammond, Orr, & Turbide, 1987). However, recent observations confirm that these extracellular vesicles are originated from donor cells and can navigate through extracellular fluids for varying times and distance (Meldolesi, 2018). Subsequently, they interact with recognized target cells and undergo fusion with endocytic or plasma membranes, followed by integration of vesicle membranes into their fusion membranes and discharge of luminal cargoes into the cytosol, resulting in changes to cellular physiology (Meldolesi, 2018). The term, extracellular vesicles is currently used to refer all the secreted membrane vesicles, though they are highly heterogeneous. Based on the current knowledge of their biogenesis and their size, EVs can be generally divided into two main categories: microvesicles and exosomes (van Niel, D'Angelo, & Raposo, 2018). Although the EVs classification and nomenclature is still a matter of debate, the term microvesicle generally refers to 150 nm to 1,000-nm vesicles released by budding from the plasma membrane (Tricarico, Clancy, & D'Souza-Schorey, 2017). The term exosome refers to small EVs ranging in size from 50nm to 150 nm in diameter formed within the endocytic pathway (Kahlert et al., 2014). The term exosome should not be confused with the exosome complex, which is involved in RNA degradation (Wasmuth, Januszyk, & Lima, 2014).

In this thesis, we focus on exosomes that are recognized as excellently equipped vehicles for information transfer between cells. Per se, exosomes play a critical biological role in intercellular communication and are implicated in a broad variety of cellular activities in health and disease (Whiteside, 2016)(van Niel et al., 2018). Several studies demonstrate the involvement of intracellular communication via exosomes in the modulation of the immune system (Greening, Gopal, Xu, Simpson, & Chen, 2015), in neurodegenerative diseases (Jan et al., 2017), in cardiovascular diseases (Greening et al., 2015), in pregnancy (Mincheva-Nilsson & Baranov, 2010) and infectious diseases (Hosseini, Fooladi, Nourani, & Ghanezadeh, 2013). However, in cancer

the role of exosomes has been extensively addressed. Several studies have demonstrated that exosomes are able to mediate the interaction between cancer cells and their microenvironment and play a critical role in the cancer development (Soung et al., 2015). The exosomes biogenesis is enhanced in cancer. It has already been described that tumor cells produce and secrete many more exosomes than normal proliferating cells (Dabirao, Margolick, Lopez, & Bream, 2011; Szczepanski, Szajnik, Welsh, Whiteside, & Boyiadzis, 2011). Cancer cells actively release cancer exosomes that transport molecular and genetic information to normal or other abnormal cells (Whiteside, 2016). This horizontal transfer of information to local or distant sites promotes tumor growth and metastasis (Atay & Godwin, 2014). In fact, exosomes released by cancer cells have been denominated “oncossomes” since they carry oncogenes (Rak & Guha, 2012). They are able to transfer proteins, lipids and nucleic acids to recipient cells, regulating gene expression. However, it is still not clear whether exosomes are specifically directed to a certain cell or their uptake is a random process (Martins, Dias, & Hainaut, 2013).

1.4.1. Exosomes biogenesis

Exosomes are generated through the endocytic pathway that is involved in the internalization of extracellular ligands or cellular components, their recycling and/or their degradation (Gould & Lippincott-Schwartz, 2009)(Klumperman & Raposo, 2014). During endosome maturation, the inward budding of clathrin-coated domains in the plasma membrane leads to the formation of intraluminal vesicles (ILVs) (Stoorvogel, Strous, Geuze, Oorschot, & Schwartz, 1991) (Sato-Kuwabara, Melo, Soares, & Calin, 2015). The generation of ILVs was reported to depend primarily on the endosomal-sorting complex required for transport (ESCRT). This complex is a molecular machine composed of four complexes of proteins subunits that is active in local membrane remodelling (Colombo et al., 2013). Along with the ESCRT machinery, others associated proteins, such as Alix and ARRDC1, have been reported to participate in this process (Hurley & Hanson, 2010). The accumulation of specific cargo at the cytosolic face of endocytic membrane microdomains is driven by these associated proteins. Some of the proteins that end up being contained within ILVs are ubiquitinated (Buschow, Liefhebber, Wubbolts, & Stoorvogel, 2005). The ESCRT machinery participates in the deubiquitination of some of the sorted proteins, a process necessary for exosomes function (Hurley & Hanson, 2010)(Colombo et al., 2013).

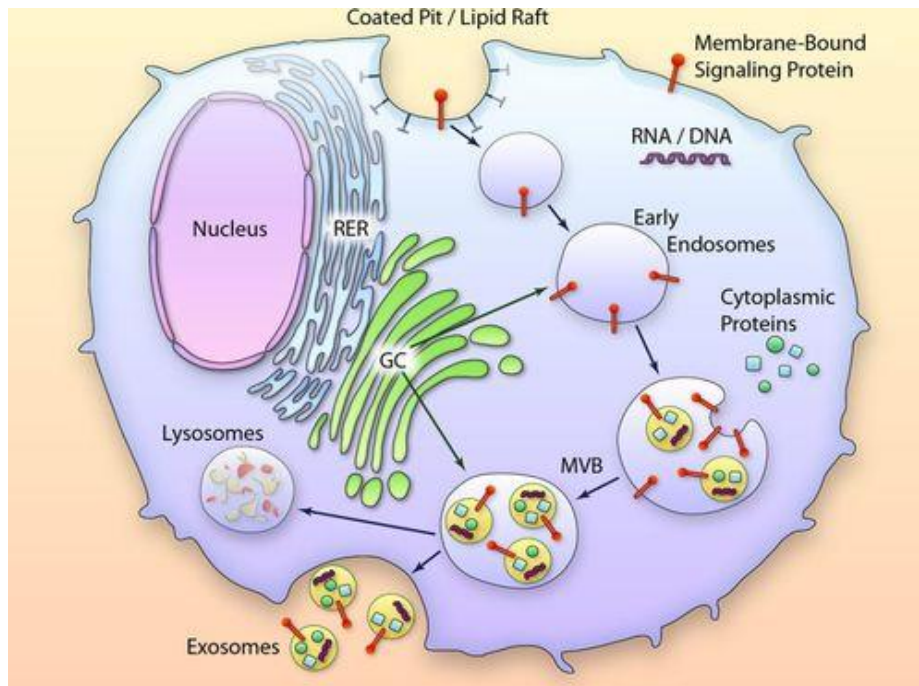


Figure 2. Exosome biogenesis and secretion. After invagination of the plasma membrane by endocytosis occurs the formation of the early endosome. During the maturation steps of the early endosome, parts of its membrane are internalised as smaller vesicles named intraluminal vesicles (ILVs), forming a multivesicular body (MVB). Simultaneously, DNA, RNA and functional proteins are encapsulated into ILVs. The fate of MVBs can be either fusion with lysosomes or fusion with the plasma membrane releasing the exosomes into the extracellular space. GC indicates Golgi complex; MVB indicates multivesicular body, and RER indicates rough endoplasmic reticulum. Adapted from Waldenström and Ronquist (2014)

Upon ILVs accumulation in the endosomal lumen, the endosomes become multivesicular bodies (MVBs) that can persist in the cytosol for variable periods of time. At some point, MVBs can either fuse with lysosomes leading to the degradation of its components or can undergo exocytic fusion with the plasma membrane releasing the ILVs (now defined as exosomes) to the extracellular space (Colombo, Raposo, & Théry, 2014). Late stages of exosome production are promoted by the Rab GTPases 27A and 27B, which mediate the fusion and docking of MVBs to the plasma membrane (Ostrowski et al., 2010). In cancer cells, the exosomes biogenesis is enhanced. It has been demonstrated that cancer cells produce and secrete more exosomes than normal proliferating cells (Dabita et al., 2011). Moreover, the levels of exosomes in plasma and other body fluids of patients with cancer are frequently elevated (Keustermans, Hoeks, Meerding, Prakken, & de Jager, 2013).

1.4.2. The composition of tumor-derived exosomes

Loads of exosomes are released by cancer cells carrying an imprint of the parent cell. Its content includes nucleic acids, proteins, enzymes, lipids, cytokines and other soluble factors, which are components of the parent cell (van der Pol, Boing, Harrison, Sturk, & Nieuwland, 2012). Regarding protein content, exosomes contain a specific subset of cellular proteins, some of which depend on the cell type that secretes them, whereas others are found in most exosomes regardless of cell type (Théry, Zitvogel, & Amigorena, 2002). The ubiquitous proteins that are present in most exosomes include proteins from endosomes, the plasma membrane, and the cellular cytosol. Interestingly, exosomes do not contain any proteins of nuclear, mitochondrial, endoplasmic-reticulum or Golgi-apparatus origin. This suggests a specificity in exosomes formation and that both ubiquitous and cell-specific proteins might be targeted selectively to exosomes (Colombo et al., 2014). As a consequence of their endosomal origin, exosomes contain a common subset of proteins that are involved in membrane transport and fusion processes such as Rab GTPases, annexins, and flotillin, components of the ESCRT complex, integrins and tetraspanins (CD9, CD63, CD81 and CD82) (Théry et al., 2002)(Kowal et al., 2016). Exosomes protein composition also include proteins involved in signal transduction, such as protein kinases, heterotrimeric G proteins and heat shock proteins (Soung, Nguyen, Cao, Lee, & Chung, 2015)(Andreu & Yáñez-Mó, 2014). Besides these common proteins, exosomes are enriched in various proteins that are specifically present in the membrane and cytoplasm of the cell of origin (Ruivo, Adem, Silva, & Melo, 2017).

In cancer, exosomes are enriched in several immunosuppressive proteins that cancer cells usually express to blunt anti-tumor immune responses (Whiteside, 2010). These proteins include death receptor (FasL or TRAIL), checkpoint receptor ligands (PD-L1), inhibitory cytokines (IL10 and TGF- β 1), as well as prostaglandin E2 (PGE2) and ectoenzymes engaged in the adenosine pathway (CD39 and D73). In addition, cancer exosomes also carry a tumor associated antigens (TAA), co-stimulatory molecules and MHC components, which enable them to stimulate immune cells and promote antitumor responses (Wieckowski et al., 2009) (Schuler et al., 2014). Several others oncoproteins are shuttled into exosomes and can modulate recipient cells upon interaction or release. Peinado et al. showed that exosomes derived from highly metastatic melanomas contain high amounts of MET oncoprotein. MET mediates cellular transformation and tumor cell proliferation, survival, motility, invasion and metastasis. The horizontal transfer of MET promotes the education and mobilization of bone marrow-derived cells (BMDCs) during pre-metastatic niche

formation (Peinado et al., 2012). Mass spectrometry analyses identified that the cell surface proteoglycan, glypican-1 (GPC1) is specifically enriched on cancer-cell-derived exosomes (Melo et al., 2015). The levels of the GPC1 present in exosomes correlate with tumor burden, making this protein a reliable biomarker for the early detection of pancreatic cancer (Melo et al., 2015). Exosomes-mediated communication is also crucial for osteosarcoma development. Cancer exosomes transfer a membrane-associated form of TGF β , which induces pro-inflammatory IL-6 production by mesenchymal stem cells. Blockade of exosomes-mediated communication hampers osteosarcoma progression (Baglio et al., 2017).

Regarding lipid content, exosomes membranes are characterized by high concentrations of cholesterol, phosphatidylserine and sphingomyelin, together with ceramide (Llorente et al., 2013)(Wubbolts et al., 2003). In addition, exosomes membranes lipids also include lysobisphosphatidic acid, an unconventional phospholipid that contributes to the accumulation of cholesterol and is absent in other cellular membranes (Chevallier et al., 2008). Exosomes present a specific lipid composition, with some features (e.g., sphingomyelin and cholesterol) reminiscent of detergent-resistant subdomains of the plasma membrane called lipid rafts (Ikonen, 2001). These results go in accordance with the presence of lipid raft-associated proteins, such as GPI-anchored proteins and flotillins, and the observed resistance of B cell exosomes to detergents (Wubbolts et al., 2003). These observations show that the lipid composition of exosomes and secreting cells is different and suggest the presence of a mechanism that sorts these specific lipids into the vesicles (Colombo et al., 2014).

The presence of nucleic acids in exosomes was first described in exosomes secreted by mast cells (Valadi et al., 2007). The presence of essentially small RNA, including mRNA, and miRNA in exosomes was then observed and confirmed by several other groups (Colombo et al., 2014). One of the most interesting discoveries concerning the presence of nucleic acid in exosomes is that they are exported outside cells and can affect gene expression in distant cells. Interestingly, it was described that exosomes derived from breast cancer cells are able to perform cell-independent miRNA biogenesis (Melo et al., 2014). In this study, the authors showed that exosomes can contain miRNAs associated with the RISC loading complex that processes pre-miRNAs into mature miRNAs.

These cancer exosomes are able to alter the transcriptome of target cells in a Dicer-dependent manner, stimulating non-tumorigenic epithelial cells to form tumors (Melo et al., 2014). Observations that different mRNA sequences are either sorted into exosomes while others are

retained inside the cells suggests the existence of different mechanisms of RNA cargo selection. In fact, a bioinformatic analysis of exported RNA sequences unravelled a putative RNA export sequence (Batagov, Kuznetsov, & Kurochkin, 2011), however, its export function has not been experimentally confirmed. More recently, it was described the presence of DNA in tumor exosomes, being the majority double-stranded DNA (Thakur et al., 2014). In a study using genomic DNA from exosomes derived from pancreatic cancer cell lines and serum from patients with pancreatic cancer, it was possible to detect mutations in KRAS and p53 (Kahlert et al., 2014).

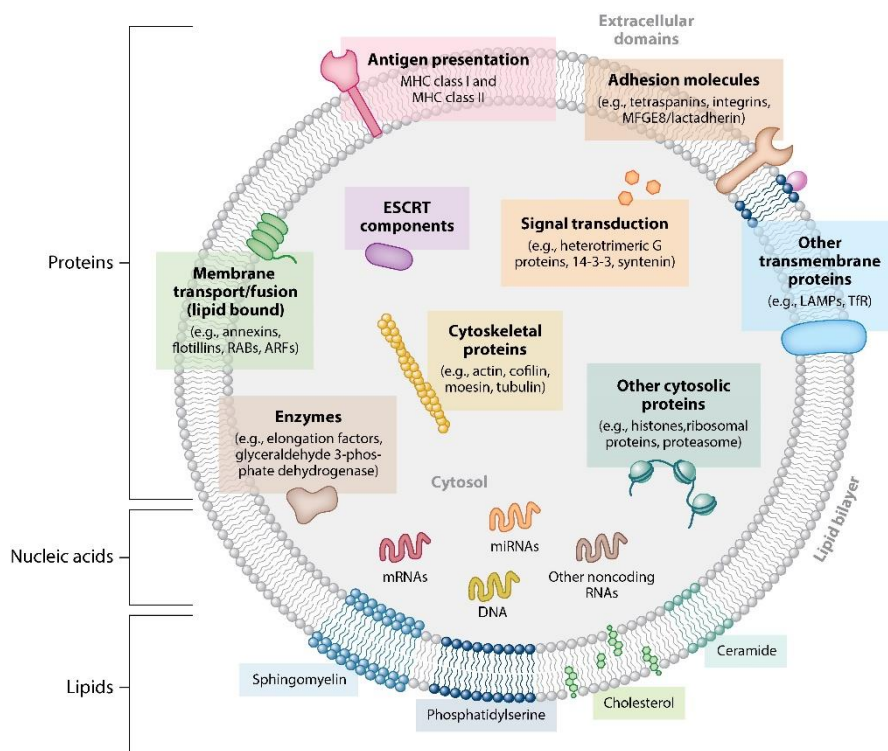


Figure 3. Schematic representation of the families of proteins, nucleic acids and lipids present in exosomes. Exosomes membrane is enriched in different lipids similar to those present in the membranes of the originating cells. Due to the endocytic origin of exosomes, they contain an evolutionary-conserved common set of proteins derived from the endocytic system, plasma membrane and cytosol as well as cell-specific proteins. Exosomes also carry nucleic acids that include DNA, mRNA and micro RNA. Adapted from (Colombo et al., 2014) (Whiteside, 2016)

Tumor cells produce exosomes with a distinct molecular profile equipped to interact with blood vessels, stromal elements and immune cells in order to establish a pre-metastatic niche. This ability of tumor-derived exosomes to support metastasis may be accomplished by engaging different molecular pathways (Whiteside, 2016).

1.4.3. Exosomes in PDAC metastasis

Exosomes represent a unique form of communication between cells that operate at short and long distances. They are present in the circulation and have access to all parts of the body and only a fraction of total exosomes present in plasma of cancer patients are cancer exosomes (Whiteside, 2016). It has been shown that the formation of pre-metastatic niches depends on tumor-derived exosomes (Hood, San, & Wickline, 2011; Peinado et al., 2012). In pancreatic cancer, there are some studies that analyse specifically the role of pancreatic cancer exosomes in metastasis, more particularly, in pre-metastatic niche formation. Costa-silva et al. presented a detailed analysis of the sequential steps of liver pre-metastatic niche formation by PDAC-derived exosomes (Costa-silva et al., 2015). Exosomes derived from malignant pancreatic lesions containing the macrophage migration inhibitory factor (MIF) selectively captured by Kupffer cells (KCs) in the liver. The exosomal MIF induces the release of transforming growth factor (TGF) by KCs, which, in turn, promotes fibronectin (FN) production. Fibronectin deposits subsequently promote the arrest of bone marrow-derived macrophages and neutrophils in the liver. Together, these events complete the formation of the pre-metastatic niche. Interestingly, the knockdown of MIF prevents all sequential steps in liver pre-metastatic niche formation, blocking the PDAC metastasis induced by cancer exosomes (Costa-silva et al., 2015).

Cancer exosomes are present in the circulation and have access to all parts of the body. Exosomes first permeabilize vessels, allowing for exosomes diffusion before being uptake by parenchymal cells (Peinado et al., 2012). They carry surface components that enable contact with endothelial cells and facilitate exosomes entry into vessels and tissues (Al-Nedawi, Meehan, Kerbel, Allison, & Rak, 2009; Skog et al., 2008; Whiteside, 2016). It has been shown that tumor-derived exosomal molecules direct exosomes to specific organs and promote organ-specific metastasis. This because exosomes from different cancer recapitulate the organ specificity of their cell of origin and prepare premetastatic niches (Hoshino et al., 2015). Hoshino et al. demonstrated that cancer exosomes determine organotropic metastasis through specific molecules in their surface, integrins, that mediate interaction with resident cells in a specific manner (Hoshino et al., 2015). They proved that exosomes derived from cancer cells with tropism for specific organs (lung, liver and brain) fuse preferentially with resident cells at their predicted destination, namely lung fibroblasts and epithelial cells, liver Kupffer cells and brain endothelial cells. Quantitative mass spectrometry analysis showed that integrins were the most abundant adhesion molecules present in exosomes. They were able to identify a correlation between exosomal integrins and metastatic organotropism,

indicating that integrins were responsible for organ-specific uptake of exosomes. Moreover, manipulation of the integrin cargo packaged into exosomes impacts metastatic organotropism (Hoshino et al., 2015). They suggested that circulating tumor-derived exosomes may be useful not only to predict metastatic propensity but also to determine organ sites of future metastasis.

1.5. Rationale

Pancreatic cancer (PC) is one of the major causes of cancer-associated mortality (Kleeff et al., 2016). Despite continuous research efforts, the incidence of PC is rising, and the overall prognosis of PC patients remains extremely poor (Siegel, Ma, Zou, & Jemal, 2014). The poor prognosis associated with pancreatic cancer is largely attributed to the fact that, by the time it is diagnosed the patient already has metastasis. The knowledge about the signalling events that mediate the progression from pancreatic cancer precursors to invasive, metastatic tumors is extremely limited (Sohn & Yeo, 2000).

In pancreatic cancer, the CXCR4/CXCL12 axis has been implicated in almost every aspect of tumorigenesis, especially in the invasive and metastatic process (Sleightholm et al., 2017). CXCR4 is expressed in several pancreatic cancer cell lines, however, its expression is higher in cell lines originated from metastatic or ascitic lesions, compared with cell lines derived from primary tumors (Marchesi et al., 2004). Emerging evidence suggests that CXCR4/CXCL12 axis facilitate the spread of migrating tumor cells expressing CXCR4 towards gradients of CXCL12 and homing to specific organs (Balic et al., 2012; Marchesi et al., 2004; Sleightholm et al., 2017). Interestingly, CXCL12, the specific ligand for CXCR4, is strongly expressed in lung, liver, bone marrow, and lymph nodes that represent the most common sites of metastasis in pancreatic cancer (S Singh et al., 2010). This suggests a mechanism analogue to the directed homing of leukocytes where these gradients of CXCL12, provide chemotactic, survival, and proliferative signals that guide implantation and support growth in these tissues (Sleightholm et al., 2017).

Moreover, recent discoveries revealed that cancer cells release soluble factors that induce the formation of microenvironments in distant organs that are beneficial to the survival and outgrowth of tumor cells before their arrival at these sites (Peinado et al., 2017). Recently, it was demonstrated that exosomes are one of the tumor-derived factors and that the formation of pre-metastatic niches depends on tumor-derived exosomes (Hood, San, & Wickline, 2011; Peinado et al., 2012). Exosomes represent a unique form of communication between cells that operate at short and long distances. They are present in the circulation and have access to all parts of the body (Whiteside, 2016). Cancer exosomes present organ specificity since they are able to recapitulate the organ specificity of their cell of origin. The surface components present in exosomes, such as integrins, are responsible for this organotropism, however, the mechanism that determines the fate of exosomes to specific metastatic sites is not fully understood.

Taken this together, we hypothesized that the chemokine receptor CXCR4 is present in pancreatic cancer exosomes and facilitates their retention at CXCL12-enriched organs to promote effective metastatic colonization at those organs.

1.6. Work plan and aims

The present work was developed in the scope of my 2nd year of the Master Course in Molecular Genetics at the Department of Biology, University of Minho, Braga. The experimental work was performed at the Genetic Dynamics of Cancer Cells Group at the i3S - Instituto de Investigação e Inovação em Saúde, University of Porto, Porto, under the supervision of Professor Sónia Melo.

We hypothesize that the presence of CXCR4 in cancer exosomes facilitates their retention at CXCL12-enriched organs promoting effective metastatic colonization at those organs. To test our hypothesis, we set some specific objectives that comprise:

- Identify the biodistribution of CXCR4+ pancreatic cancer exosomes *in vivo*;
- Determine the role of CXCR4 in the *in vivo* distribution of pancreatic cancer exosomes;

The outcome of the present work may contribute with new insights into the emerging role of exosomes in cancer and to the understanding of the biological relevance of CXCR4 in pancreatic cancer progression and metastasis.

2.MATERIAL AND METHODS

2.1. Cell culture

Two PDAC cell lines, MIA PaCa-2 and PANC-1, originally obtained from ATCC, were used in this study. MIA PaCa-2 cell line is derived from a human pancreatic adenocarcinoma characterized by two different cell populations, one with an adherent epithelial morphology and another with a non-adherent mesenchymal morphology. PANC-1 cell line is derived from a human pancreatic ductal adenocarcinoma and has an adherent epithelial morphology. Cell lines were thawed from cryopreserved vials stored in liquid nitrogen. Cells were maintained in RPMI 1640 (1X) medium (Gibco), supplemented with 10% of FBS (Fetal Bovine Serum) (Gibco), and 1% penicillin-streptomycin (Gibco) in a 5% CO₂ humidified incubator at 37°C.

2.2. pEYFPCXCR4-N1 plasmid expansion

The pEYFPCXCR4-N1 (CXCR4-EYFP) plasmid, kindly provided by Doctor Richard J. Miller from Feinberg School of Medicine, Northwestern University, Chicago (Toth, Ren, & Miller, 2004), harbors the EYFP fluorescent protein fused to the C-terminal end of the rat CXCR4.

Plasmid expansion was achieved by transforming the TOP10 Competent Cells provided by the Cell Division Mechanisms group of i3S. After mixing the DNA with competent cells, the transformation tubes were heat shocked at 42°C for 45 seconds. Then, bacteria were incubated in LB medium (NZYTech) without any antibiotic in a 37°C shaking incubator for 45 minutes. Subsequently, bacteria were plated in the LB agar (NZYTech) plates containing kanamycin (1µL /mL) and incubated overnight at 37°C. A single colony was taken from the plate and transferred to LB liquid medium with kanamycin (1µL /mL). Bacteria were incubated overnight at 37°C in agitation. To extract and purify the plasmids of interest, ZymoPURE™ Plasmid Midiprep kit (Zymo Research) was used according to the manufacturer's protocol. DNA concentration and purity of the plasmid were measured at 260 and 280 nm using the NanoDrop® ND-1000 spectrophotometer.

2.3. Cell line transfection

MIA PaCa-2 and PANC-1 were transiently transfected with the CXCR4-EYFP plasmid (2µg DNA/5 × 10⁵ cells) using Invitrogen Lipofectamine® 2000 (Invitrogen) according to the manufacturer's instructions. The transfected cells were selected by cell sorting using the FACS Aria

sorter (Advanced Flow Cytometry Unit of i3S, Porto). Cells were cultured in selection medium containing 1mg/mL of G418 (Biowest) in a 5% CO₂ humidified incubator at 37°C.

2.4. Exosomes isolation

2.4.1. Cell culture media

To isolate exosomes from cell culture medium, 70% to 80% confluent cells were cultured in exosomes-free medium (RPMI medium supplemented with 10% FBS depleted of exosomes and 1% PenStrep). Cells were maintained in a humidified incubator with 5% CO₂ at 37°C. After 72 hours the conditioned medium was collected and centrifuged at 2500g for 10 minutes followed by a centrifugation at 4000g for 5 minutes. Then, medium was filtered (Pore size: 0.22µm) directly to an ultracentrifuge tube and the volume was topped with PBS1X (Fisher BioReagents). To obtain an exosomes pellet, the samples were centrifuged overnight at 100000g, 4°C (Beckman Optima L80-XP). The supernatant was carefully removed, and the pellet was resuspended in 100 µl of PBS1X. Samples were diluted in PBS1X (1:500) and their size and concentration were measured using NanoSight NS300 particle counter.

2.4.2. Serum

To isolate exosomes from the serum of KPC (*Kras*^{G12D/+}; *TP53*^{R172H/+}; *Pdx-1*^{Cre/+}) animals, the serum was diluted in PBS1X and filtered (Pore size: 0.22µm) to an ultracentrifuge tube. The volume was completed with PBS1X and samples were centrifuged overnight at 100000g, 4°C (Beckman Optima L80-XP). The supernatant was carefully removed, and the exosomes pellet was resuspended in 100 µl of PBS. Samples were diluted in PBS1X (1:500) and their size and concentration were measured using NanoSight NS300 particle counter.

2.5. Flow cytometry analysis

2.5.1. Cells

To determine the levels of CXCR4 in MIA PaCa-2 and PANC-1 cell lines, cells at 80-90% confluent were trypsinized, using 0.05% (w/v) Trypsin-EDTA (0.5%) trypsin-EDTA (1×) (Gibco) and counted using Trypan Blue Solution, 0.4% (Gibco) and TC20™ Automated Cell Counter (BIO-RAD).

2.5.1.1. Membrane

To determine the membrane protein levels of CXCR4 and CD133, cells were initially blocked using 10% FBS (Gibco) for 15 minutes. Then, cells were incubated with the primary antibody anti-CXCR4 (dilution 1:50, abcam) in 2% FBS for 45 minutes. After washing cells 3X using PBS1X, cells were incubated for 30 min with the secondary antibody anti-IgG goat Alexa-Fluor® 488 in 2% FBS (dilution 1:200, Invitrogen). After washing cells 3X using PBS1X, cells were incubated with the antibody anti-CD133 conjugated with PE-Vio770 (dilution 1:4, Miltenyi Biotec) antibody in 2% FBS for 30 minutes. After washing cells 3X using PBS1X, cells were then transferred to FACS tubes and analysed at BD FACSCanto™ II (BDBiosciences). As control we used secondary antibody only.

2.5.1.2. Intracellular

To determine the intracellular levels of CXCR4, cells were fixed in 4% paraformaldehyde (PFA) (Sigma-Aldrich) for 15 minutes. Afterwards, a 5 minutes incubation with 0.1%Triton/PBS1X was performed for permeabilization. Cells were then blocked in 5% BSA/PBS1X/0,1%Triton for 30 minutes. Cells were incubated with the primary antibody anti-CXCR4 (dilution 1:50, Abcam) in 2% BSA/PBS1X/0,1%Triton for 45 minutes. After washing cells 3X with PBS1X/0,05%Triton, cells were incubated for 30 min with the secondary antibody anti-IgG goat Alexa-Fluor® 488 in 2% BSA/PBS1X/0,1%Triton (dilution 1:200, Invitrogen). After washing cells 3X using PBS1X/0,05%Triton, cells were then transferred to FACS tubes and analysed at BD FACSCanto™ II (BDBiosciences).

2.5.2. Exosomes

2.5.2.1. Exosomes from cell culture medium

To determine the levels of CXCR4 and CD133 in MIA PaCa-2 and PANC-1-derived exosomes, their size and concentration was measured using nanoparticle-tracking analysis (NanoSight NS300 particle counter). Exosomes were incubated overnight at 4°C with aldehyde/sulfate latex beads (Alfagene) in a proportion of 5 µL of beads per 8×10^{10} exosomes. On the next day, exosomes were incubated with glycine 1M for 1 hour on a rotator. Then, exosomes were blocked in 10% BSA/PBS1X for 45 minutes at room temperature. Exosomes were incubated with the primary antibody anti-CXCR4 (dilution 1:50, Abcam) in 2% BSA/PBS1X for 45 minutes. After washing the

exosomes 3X with PBS1X, a 30 minutes incubation with the secondary antibody anti-IgG goat Alexa-Fluor® 488 in 2% BSA/PBS1X (dilution 1:2000, Abcam) was performed. After washing 3X with PBS1X, exosomes were incubated with the antibody anti-CD133 conjugated with PE-Vio770 in 2% BSA/PBS1X (dilution 1:4, Miltenyi Biotec) for 30 minutes. Samples were then transferred to FACS tubes and analysed using the BD FACSCanto™ II (BDBiosciences).

2.5.2.2. Exosomes from serum samples

To determine the levels of CXCR4 in serum exosomes, their size and concentration was measured by nanoparticle tracking analysis (NanoSight NS300 particle counter). Exosomes were incubated for 1 hour at 4°C with aldehyde/sulfate latex beads (Alfagene) in a proportion of 5 µL of beads per $3,0 \times 10^9$ exosomes. Exosomes were incubated with glycine 1M for 1 hour at room temperature and blocked in 10% BSA/PBS also for 1 hour at room temperature. Exosomes were incubated with the primary antibody anti-CXCR4 (dilution 1:50, Abcam) in 2% BSA/PBS overnight at 4°C. Exosomes were washed 3 times and incubated for 30 min with the secondary antibodies anti-IgG goat Alexa-Fluor® 488 in 2% BSA/PBS (dilution 1:2000, Abcam). After washing 3 times, samples were transferred to FACS tubes and analysed using the BD FACSCanto™ II (BDBiosciences).

2.6. Protein extraction and quantification

To extract protein from adherent cells, culture medium was removed, and cells were washed with PBS1X and ice-cold RIPA buffer (Amersco) supplemented with protease inhibitor cOmplete (Roche) and phosphatase inhibitor phenylmethanesulfonyl fluoride (Sigma-Aldrich) were added. Using a plastic cell scraper adherent cells were scraped off the flask. The cell lysates were incubated on ice for 30 minutes following a 30 minutes centrifugation at 17000 g, 4°C. The supernatant was transferred to a fresh tube and the pellet was discarded.

To extract protein from exosomes, after an overnight ultracentrifugation, the pellet was lysed in 8M urea and 2.5%SDS and incubated on ice for 30 minutes, followed by a 30 minutes centrifugation at 17000 g, 4°C.

Total protein concentrations were determined using an adaptation to the Lowry's method (DC™ Protein Assay Reagent, BIO-RAD) according to the manufacturer's instructions.

2.7. Western blot

Prior to gel electrophoresis, 25µg of the different protein samples were incubated with laemmli buffer (ratio 4:1) for 10 minutes at 95°C. For CXCR4 western blot, laemmli buffer was not supplemented with β-mercaptoethanol. Proteins were separated by 10% (w/v) sodium dodecyl sulphate (SDS)-polyacrylamide gel electrophoresis at 150V and 25mA until the protein of interest was conveniently separated. The molecular weight estimation of the obtained bands was made using Precision Plus Protein™ Dual Color Standards (BIO-RAD). After proteins were transferred onto nitrocellulose membranes 0.2µm (GE Healthcare) using a wet electrophoretic transfer for 90 minutes at 100V. Ponceau was added in order to confirm an effective protein transfer and for loading control in western blots where protein derived from exosomes was analysed. The nitrocellulose membranes were then blocked for 1 hour at room temperature with 5% non-fat dry milk in PBS1X/0.1% Tween 20 to block nonspecific binding sites on membranes. After blocking, membranes were incubated overnight on a shaker at 4°C with following primary antibodies in 2% non-fat dry milk in PBS/0.1% Tween 20: anti-GFP (dilution 1:500, Abcam), anti-CXCR4 (dilution 1:500, Abcam) and anti-actin (dilution 1:10000, Sigma-Aldrich). After 4 washes for 10 min intervals on an orbital shaker with PBS1X/0.1% Tween 20, membranes were incubated with horseradish peroxidase (HRP)-conjugated secondary antibodies: anti-chicken (1:5000, Sigma) and anti-rabbit (1:2500, Sigma) were incubated for 1h at room temperature. After 4 washes for 10 min intervals on an orbital shaker with PBS1X/0.1% Tween 20 membranes were incubated with Clarity™ Western ECL Substrate (BIO-RAD), according to the manufacturer's recommendations. Bands were detected using development using GE Healthcare Amersham™ Hyperfilm™ ECL (GE Healthcare).

2.8. *In vitro* co-culture

A lamella was placed inside a 6-well plate. Fresh medium was added and 200.000 PANC1 CXCR4-EYFP and PANC1 CD81-Tomato cells were mixed and plated in a proportion of 1:1. The co-culture was maintained in a 5% CO₂ humidified incubator at 37°C for 72 hours. Cells were washed with cold PBS1x and fixed in 4% PFA for 15 min at room temperature. After 2 washing steps with PBS1X for 10 minutes, cells were incubated with Hoechst solution in PBS1X (dilution 1:10 000, Thermo Scientific) for 10 minutes. Then, the lamella was mounted using a drop of Prolong Diamond

Antifade Mountant (Invitrogen). Samples were kept at 4°C protected from light until observation at the spectral confocal microscope Leica TCS-SP5 AOBs (Bioimaging Centre, i3S, Porto).

2.9. KPC mice euthanasia

KPC mice were euthanized at 27 weeks. One hour prior to euthanasia, 100µL of FITC-Dextran 2000 (Sigma-Aldrich) was injected retro-orbitally and pimonidazole (60mg/kg) (Hypoxic Probe) was injected intraperitoneally. At the time of euthanasia, animals were anaesthetised in 4% isoflurane and all the blood was collected retro-orbitally followed by cervical dislocation. The abdominal cavity was exposed, and necropsy was performed. The pancreas, lung, liver, lymph nodes, spleen, kidneys, muscle and duodenum were collected and placed in formalin 20% v/v for tissue fixation. Tissue from each organ was also snap frozen.

2.10. H&E stain

4µm cuts were performed using a paraffin microtome Microm HM335E (HEMS, i3S, Porto) and transferred to KP frost slides (Klinipath). Slides were incubated at 37°C overnight. Sections were then stained using the hematoxylineosin staining. Samples were dewaxed with xylene, followed by submersion in solutions with decreasing concentrations of alcohol (100%, 100%, 70%) and then rinsed with running water to hydrate. After staining with Modified Gill II Hematoxylin (Merck Millipore, Burlington, MA, EUA) and differentiation with running water, the sections were dehydrated using solutions with increasing concentrations of alcohol (70%, 100%, 100%) and then stained with an alcoholic eosin solution (Thermo Scientific), quickly rinsed in 100% ethanol and then diaphanized twice with xylene. Samples were then mounted using DPX mounting medium (Sigma-Aldrich) a glass coverslip (Normax). To visualize the staining, an optical microscope was used.

2.11. Immunohistochemistry (IHC)

4µm cuts were performed using a paraffin microtome Microm HM335E (HEMS, i3S, Porto) and transferred to coated slides (Thermofisher). Slides were incubated at 37°C overnight. The

standard protocol used was as follows were dewaxed with xylene, followed by submersion in solutions with decreasing concentrations of alcohol (100%, 100%, 70%) and then rinsed with running water to hydrate. Samples were then subjected to antigen retrieval by putting the slides in an antigen unmasking solution, 1 μ M EDTA pH8 (Sigma-Aldrich), into a water vaporizer machine at approximately 99°C for 25 minutes. Afterwards, slides were left at room temperature (RT) for 20 minutes to cool down and then washed twice in PBS1X/0.1% Tween 20 for 5 minutes, with gentle agitation. The next step was the inactivation of tissue endogenous peroxidase by incubation of the slides for 15 minutes in a 3% hydrogen peroxide in methanol solution (H_2O_2 [Sigma-Aldrich]; CH_3OH [VWR]) and washed in PBS1X/0.1% Tween 20 twice as previously mentioned. Tissue sections were delimited using a hydrophobic pen (Vector Labs) and incubated with Ultravision Protein-block solution (Thermofisher), using enough volume to cover the tissue section, for 15 minutes at RT. Slides were then incubated with the anti-CXCR4 antibody (1:500) diluted in ready to use Antibody diluent OP Quanto (Thermofisher) in a humidified chamber overnight at 4°C. For each sample, a negative control was performed, in which, instead of adding primary antibody, PBS1X was used. The next day, slides were washed in PBS1X/0.1% Tween 20 twice for 5 minutes, with gentle agitation to remove the excess of primary antibody. Afterwards, REAL EnVision detection system kit (Dako) was used for signal detection. The kit includes an HRP-anti IgG rabbit/mouse universal secondary antibody that was added to the tissue followed by an incubation of 30 minutes at RT in the humidified chamber. A new wash with PBS1X/0.1% Tween 20 was performed as described above. Dako REAL™ Diaminobenzidine (DAB) positive chromogen, which produces a brown staining at the site of reaction, was used. Slides were incubated with DAB until a brown color first became visible on the sections for one minute. The reaction was stopped by washing slides in running water for 5 minutes. The counterstain (to stain the nucleus) was performed by incubating the slides in hematoxylin for 2 minutes, followed by a washing step in running water for 5 minutes. Slides were then dehydrated with ethanol (5 minutes in 100% ethanol and two rounds of 5 minutes in 70% ethanol solutions) followed by incubation in xylene solution (two rounds of 5 minutes), Finally, slides were mounted with DPX mounting medium (Sigma-Aldrich). Slides were then analysed under the optical microscope.

2.12. Orthotopic injection of PANC-1 CXCR4-EYFP cells

Cells were grown under normal conditions up to 70% confluence upon which they were trypsinized. Using the Trypan Blue Assay and a haemocytometer the number of cells and their viability was assessed. The desired number of cells were resuspended in a mixture of matrigel and saline solution (3:2). The matrigel-cell suspension was maintained on ice until injection.

For this experiment 24 Rag2^{-/-}; Il2rg^{-/-} immunodeficient mice were used. The mice were weighed and anaesthetized by intraperitoneal administration of a ketamine (125mg/kg)/xylazine (12.5mg/kg) solution. As an analgesic, buprenorphine (0.08 mg/kg) was injected subcutaneously. After shaving the mice hair, the left side of abdominal skin was sterilized by painting the area with betadine solution, and then with 70% ethanol. A small incision in the left abdominal flank was made and the pancreatic tissue was exposed. Using a Hamilton syringe the cell suspension maintained in ice was resuspended. The needle was inserted into the pancreas and the 20µl of cell suspension containing 3.5x10⁶ cells was slowly injected. The pancreas was carefully returned to the peritoneal cavity and the abdominal muscle layer and the skin layer were sequentially closed with interrupted 6-0 PGA sutures (Surgicryl PGA 6-0). After surgery, the anaesthetic effect was reversed by subcutaneous administration of atipamezole (2.5mg/kg). In the next day, another dose of analgesic was administered to the animals. After tumor implantation, all mice were monitored at least twice weekly for the tumor growth and general signs of morbidity such as ruffled fur, hunched posture, and immobility.

2.13. Matrigel Plugs *in vivo* experiment

200 µL of Matrigel Growth Factor Reduced and Phenol Red-free (Corning®) plugs supplemented with 200 ng/mL recombinant murine CXCL12 (PeproTech) were prepared for subcutaneous implantation in Rag2^{-/-}; Il2rg^{-/-} immunodeficient mice (n=20). As controls, Matrigel plugs supplemented with H₂O were used. Briefly, Matrigel was used according to the manufacturer's instructions and supplemented with each of the components for each group. Matrigel is liquid at 4°C, however Matrigel at room temperature (RT) polymerises producing a gel. The matrigel mixture containing either the CXCL12 or water were maintained on ice. A plastic flat surface and the round support to make the plugs with the same dimensions were maintained under a heating pad. Around 30 minutes before plug implantation, 200µL of Matrigel containing 200 ng/mL of CXCL12 or H₂O

was transferred to the heated support and were allowed to polymerise. Meanwhile, mice were anaesthetized with 4% isoflurane in an induction chamber and maintained with 2,5% isoflurane. Plugs were placed in two separate subcutaneous pockets. The plug containing the recombinant CXCL12 was placed in the right flank near the shoulder and the control plug was placed in the lower right flank, both equidistant from the pancreas. The animals were postoperatively treated with the analgesic buprenorphine subcutaneously (0.05 mg/kg).

The 20 animals containing PANC-1 CXCR4-EYFP tumors, were randomized into 4 groups subjected to different treatments. The treatments started 1 day before the plugs were implanted and were performed daily for 5 days. At day 6, animals were euthanised. One group was treated daily with a rabbit polyclonal neutralizing antibody to CXCR4 (Torrey Pines Biolabs) (0.4 mg/kg) injected intraperitoneally (n=5) or with IgG control antibody (0.4 mg/kg) injected intraperitoneally (control, n=5). The other group was treated daily with 1.25 mg/kg of GW4869 in 2.5% DMSO injected intraperitoneally (n=5) or 2.5% DMSO in saline solution (control vehicle, n=5).

2.14. Procedure for mice euthanasia

Animals were anaesthetized by intraperitoneal injection of a Ketamine (150 mg/kg)/Medetomidine (2 mg/kg) solution. When no tail reflex was observed, Matrigel plugs were carefully removed from the animals. The rCXCL12 and control plugs were placed in a black surface previously identified and the levels of fluorescence were measured using the IVIS Spectrum CT In Vivo Imaging System. After the matrigel plug removal, the animal was placed in a grid and sprayed with 70% ethanol. A small incision on the skin right below the sternum all the way up until the chin was performed and the rib cage was fully exposed. The tip of the sternum was pinched, and a small cut was made. The ribs were removed, and heart was exposed. After ensuring the peristaltic pump had no air bubbles a needle was placed on the edge of the tube. Then, using minimal aggressive forceps (round edges) the heart was pinched, the needle was injected on the bottom of the left ventricle and the vein above the right aorta was cut.

The peristaltic pump was turned on (level 6) to inject 20mL ice-cold PBS1X. Using a 2mL syringe containing heparin, blood was collected. After finishing the 20mL of PBS1X, peristaltic pump was turned off and changed to 4% PFA pH 7,4. 17,5 mL of 4% PFA were injected. After the transcardial perfusion, animal dissection was performed. The organs collected were: pancreas/tumor, spleen, lymph nodes, kidneys, lung, liver, brain, muscle and bone. The

pancreas/tumor was measured with callipers and weighted. All organs were maintained in 4% PFA. Tissue sample from the pancreas/tumor, spleen, lung, liver, muscle and ear/tail were snap frozen. Blood was centrifuged at 2000g 10min 4°C for serum collection. Organs were maintained overnight at 4°C in 4% PFA protected from light. In the next day, organs were washed 2 times with autoclaved PBS1X and incubated in 30% sucrose overnight at 4°C, protected from light. Finally, organs are embedded in OCT and frozen in dry ice. Samples are stored at -80°C.

2.15. Imaging acquisition and processing

Tissue sections of 30 µm were obtained using a cryostat Leica CM 3050S (HEMS, i3S, Porto) and assembled in coated slides (Thermofisher), which were then incubated 30 minutes at room temperature protected from light. After 3 washing steps of 10 minutes with PBS1X, tissue sections were incubated with Hoechst solution in PBS1X (dilution 1:10 000, Thermo Scientific) for 10 minutes. Afterwards, sections were washed 3 times during 10 minutes with PBS1X. Coverslips were mounted using a drop of Prolong Diamond Antifade Mountant (Invitrogen). Samples were kept at 4°C protected from light. Samples were imaged using the 10x dry and 40x oil objectives from a spectral confocal microscope Leica TCS-SP5 AOBs (Bioimaging Centre, I3S, Porto) equipped with bright field optics. Images were acquired in 20 z-planes 1-2µm average apart, using the following lasers lines: 488nm, 561nm (20 % of the Argon Laser maximum power) and 405 nm (100 % of the maximum power). XYZ images were collected using PMT detectors in sequential mode with a format of 1024x1024 pixels and 200Hz of scanning speed.

The image processing was done in the Fiji (ImageJ) software. After obtaining the maximum projection of the different plans acquired for each plug the setting Brightness/Contrast was adjusted to reduce the background fluorescence (minimum=20, maximum=255). Using the drawing tool, plugs were delimited, and the mean intensity of fluorescence was measured considering the plug area. All images were scaled equally.

2.16. Statistical analysis

Statistical analysis of the results was performed using GraphPad Prism 7 Software (version 6).

Data for all flow cytometry analysis was performed at least three independent experiments.

The statistical analysis for the comparison between two groups was performed using an unpaired T test. The statistical analysis for the treatment experiments was performed using a non-parametric test once the number of animals in each group was not the same. Statistical significance and P-value were calculated using the Kruskal-Wallis Test and the Dunn's Multiple Comparison Test. Samples with p values under 0.05 were considered significant.

3.RESULTS

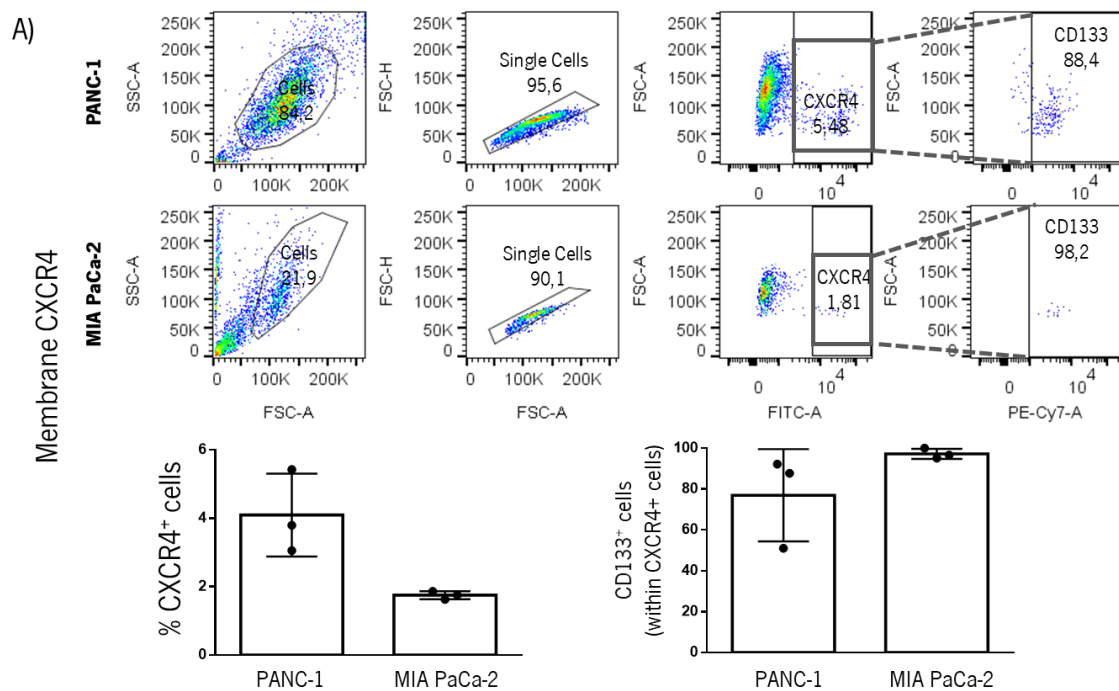
3.1. CXCR4 is expressed in PDAC cell lines and co-expresses with CD133

It is well described that CXCR4 and CD133 identify a subset of pancreatic cancer cells with stem cell-like characteristics, the cancer stem cells (CSC). These cells have higher metastatic potential (Hermann et al., 2007). We evaluated cell surface expression of CXCR4 and CD133 by flow cytometry in two PDAC cell lines, MIA PaCa-2 and PANC-1.

Membrane levels of CXCR4 in MIA PaCa-2 were 1.7% and in PANC-1 4% (**Figure 4A**). PANC-1 cells showed higher levels of membrane CXCR4 when compared to MIA PaCa-2 cells. In both cell lines there was a significant percentage of cells which were double positive for CXCR4 and CD133 marker. In MIA PaCa-2 cells 97% of CXCR4⁺ cells were also positive for CD133, while in PANC-1 cells only 76% of CXCR4 positive cells were CD133⁺ (**Figure 4A**).

CXCR4 is mainly described in the cell membrane, however, several authors describe the presence of biologically active intracellular CXCR4 (Cepeda et al., 2015). Therefore, we have also evaluated intracellular CXCR4 by flow cytometry in both cell lines. The intracellular levels of CXCR4 were 98% in MIA PaCa-2 and 97% in PANC-1 (**Figure 4B**).

In this way we have identified a subpopulation of pancreatic cancer cells that expresses membrane-associated CXCR4 that are also CD133 positive.



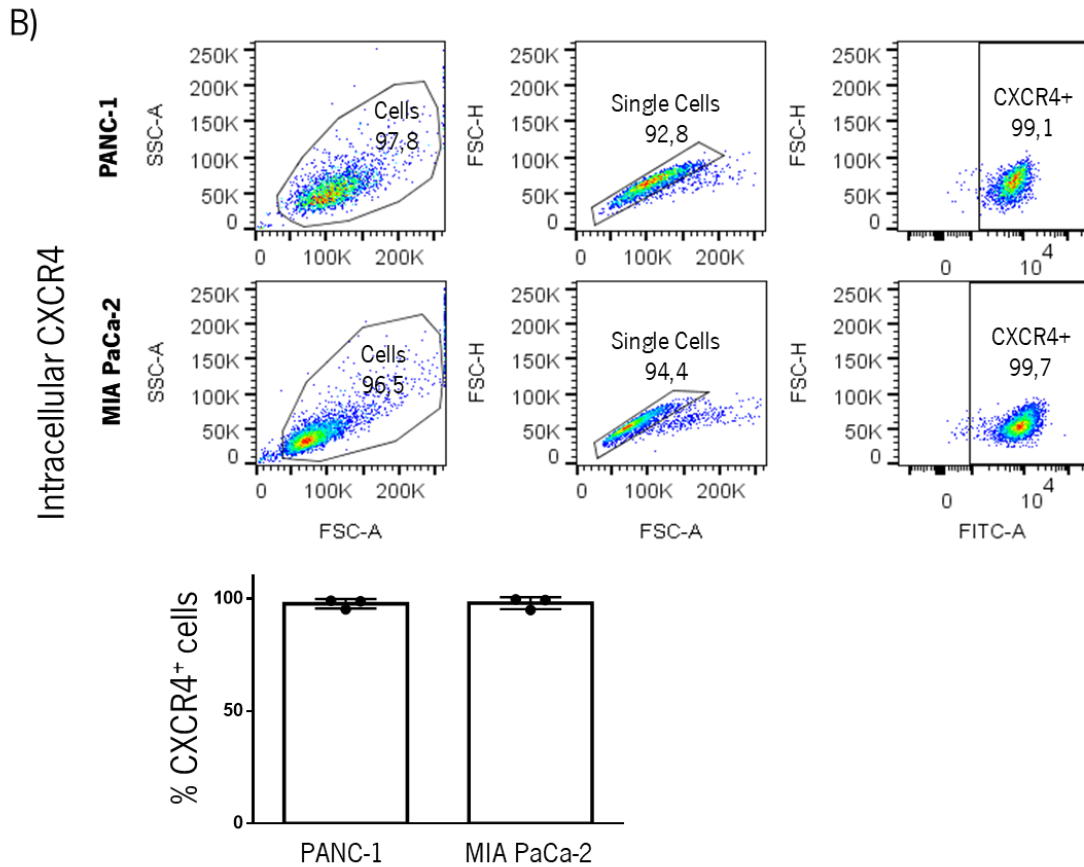
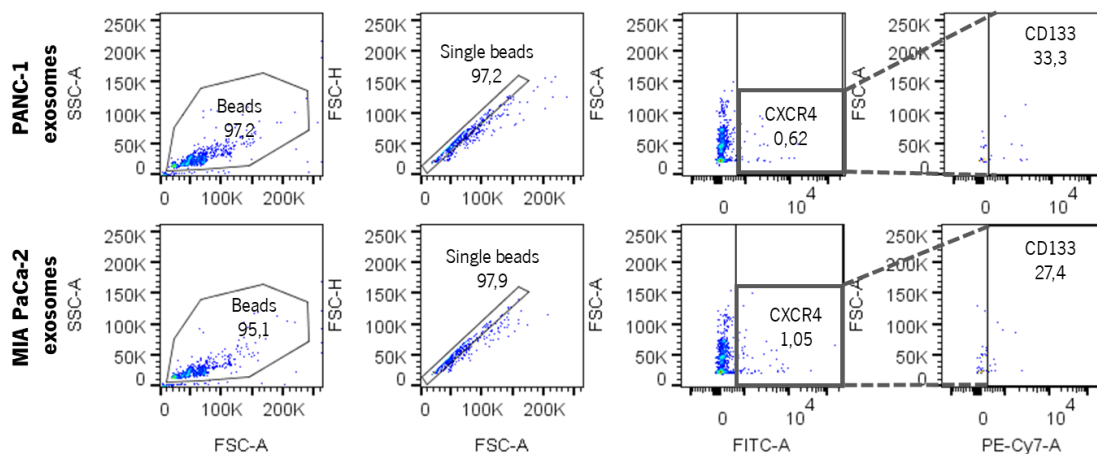


Figure 4. CXCR4 is expressed in PDAC cell lines and co-expresses with CD133 (A) Percentages of MIA PaCa-2 and PANC-1 cells positive for membrane associated CXCR4 staining and percentages of CD133⁺ cells within the CXCR4⁺ cells. MIA PaCa-2 and PANC-1 cells were stained with anti-CXCR4 and CD133 antibodies and the percentage of CXCR4⁺ cells and the percentage of CXCR4⁺ cells that express CD133 were measured using FACS Canto II. Three independent experiments were performed. Representation of the flow cytometry plots of one replicate. **(B)** Percentages of MIA PaCa-2 and PANC-1 cells positive for intracellular CXCR4 staining. MIA PaCa-2 and PANC-1 permeabilized cells were stained with anti-CXCR4 and the percentage of intracellular CXCR4⁺ cells was measured using FACS Canto II. Three independent experiments were performed. Representative CXCR4⁺ CD133⁺ cells flow cytometry plots. Cells stained with secondary antibody only were used as controls. Data shown as mean \pm SD. N=3 biological triplicates.

3.2. Exosomes of PDAC cell lines are CXCR4 and CD133 positive

Since CXCR4 and CD133 markers are present in the MIA PaCa-2 and PANC-1 PDAC cell lines, we decided to test the presence of these markers in exosomes isolated from the same cells. The

presence of CXCR4 and CD133 in exosomes-derived from MIA PaCa-2 and PANC-1 were analysed by flow cytometry coupled to latex beads. 0.6% of MIA PaCa-2 isolated exosomes are CXCR4 positive, while 0.4% of PANC-1 derived exosomes were positive for CXCR4 (**Figure 5**). Despite the slightly higher percentage of CXCR4 positive exosomes from MIA PaCa-2 cells when compared with PANC-1 exosomes, this difference was not statistically significant.



FACS analysis exosomes

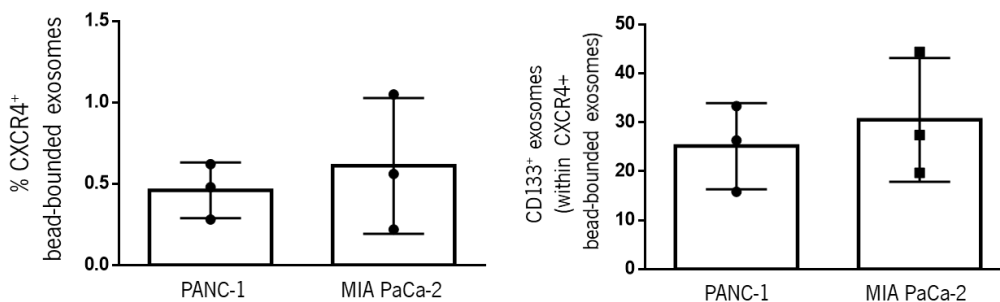


Figure 5. Exosomes of PDAC cell lines are CXCR4 and CD133 positive Percentages of MIA PaCa-2 and PANC-1 derived-exosomes positive for membrane associated CXCR4 staining and percentages of CD133⁺ exosomes within the CXCR4⁺ exosomes. Exosomes were stained with anti-CXCR4 and CD133 antibodies and the percentage of CXCR4⁺ beads and the percentage of CXCR4⁺ exosomes that express CD133 were measured using FACS Canto II. Three independent experiments were performed. Representative CXCR4⁺ CD133⁺ exosomes flow cytometry plots. Exosomes stained with secondary antibody only were used as controls. Data shown as mean ± SD. N=3 biological triplicates.

Regarding the co-expression of CXCR4 and CD133 in exosomes isolated from the referred cell lines, we observed that in MIA PaCa-2 30% of CXCR4⁺ exosomes were also positive for CD133 and

in PANC-1 25% of CXCR4⁺ exosomes were also positive for CD133 (**Figure 5**). Despite the tendency to obtain higher levels of CXCR4⁺ CD133⁺ exosomes in MIA PaCa-2 cell line when compared to PANC-1, this difference was not statistically significant.

Therefore, exosomes derived from pancreatic cancer cells contain CXCR4 membrane-associated protein and are concomitantly positive for CD133.

3.3. Establishment of CXCR4-EYFP PDAC cell lines

In order to characterize the biodistribution of CXCR4⁺ exosomes *in vivo*, we needed to develop a tool that would allow us to trace exosomes upon their secretion by cancer cells. With this purpose, CXCR4-EYFP pancreatic cancer cells were established to obtain exosomes with the receptor CXCR4 fused with a fluorescent protein (EYFP), in this way allowing *in vivo* tracking of the exosomes. MIA PaCa-2 and PANC-1 cells were transiently transfected with the pEYFP-N1-CXCR4 plasmid, containing the C-terminal end of the rat CXCR4 fused with the yellow (EYFP) version of the green fluorescent protein (**Figure 6A**). The rat protein presents an 92% homology with the human protein (Chen et al., 2014), and therefore we predict that no significant changes will be observed that concern the species from which the CXCR4 is derived. To select for transfected color-coded clones, antibiotic selection was done with G418 and cells were sorted for enrichment purposes. To confirm that the EYFP clones were stable we analysed the percentage of CXCR4-EYFP⁺ cells by flow cytometry (**Figure 6B**). In both cell lines by fluorescence microscopy, we could observe that the CXCR4-EYFP fusion protein is mainly localized in the plasma membrane, but also present in the cytoplasm and perinuclear region as previously described (Cepeda et al., 2015) (**Figure 6B**). In the PANC-1 CXCR4-EYFP cell line almost all cells express the fusion protein, although the level of expression varies among cells (**Figure 6B**). Regarding the MIA PaCa-2 CXCR4-EYFP cell line, we observe that the number of cells that express the fusion protein is lower when compared to the PANC-1 CXCR4-EYFP cells. The level of expression also varies among the different cells (**Figure 6B**). These differences are also observed by flow cytometry. The PANC-1 CXCR4-EYFP cell line was 94% EYFP⁺ and the MIA PaCa-2 CXCR4-EYFP cell line was 48% EYFP⁺ (**Figure 6B**). Therefore, we have established a model in which pancreatic cancer cells express color-coded CXCR4 protein.

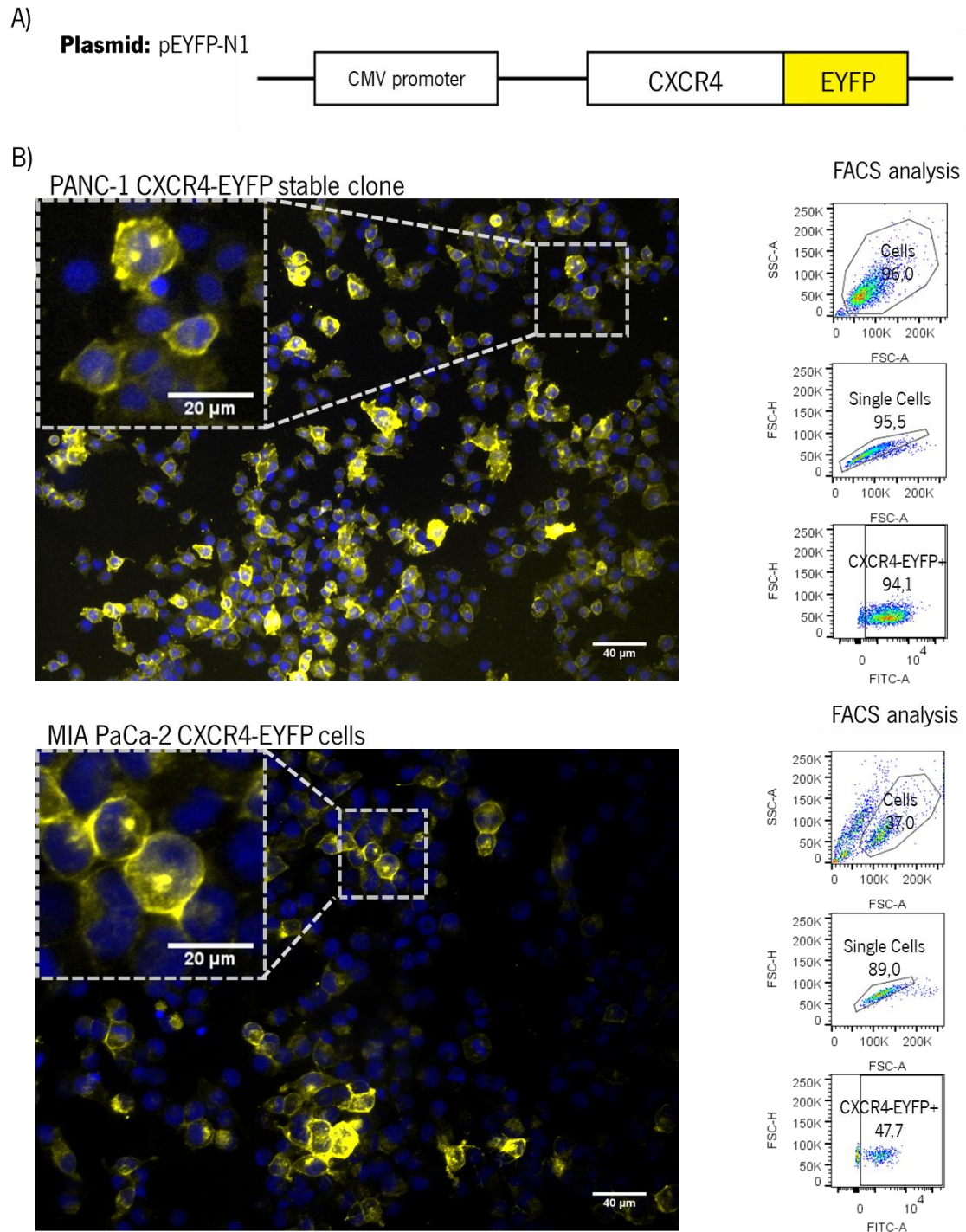
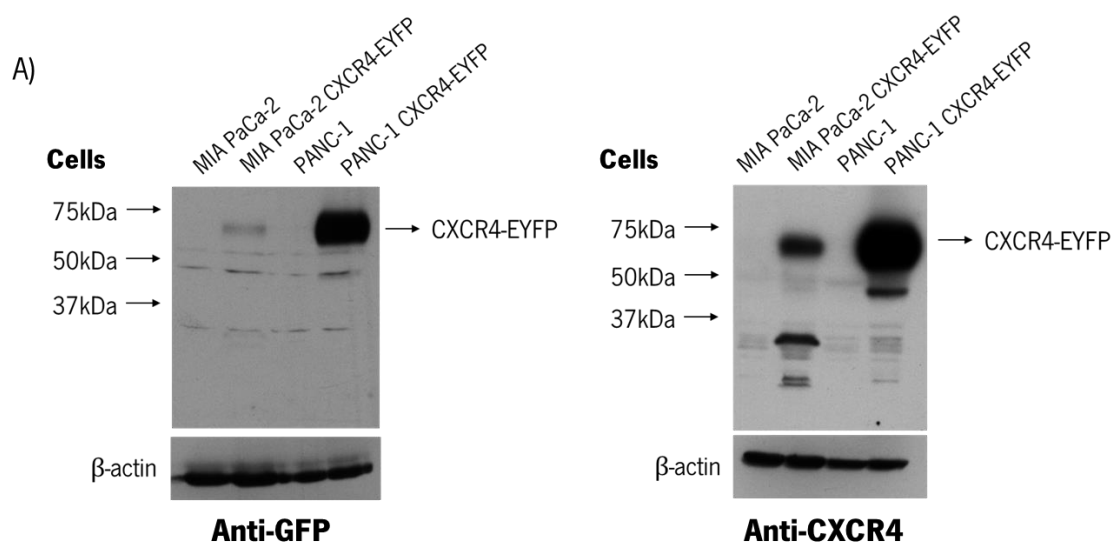


Figure 6. Establishment of CXCR4-EYFP PDAC cell lines (A) EYFP is fused to the C-terminal end of the rat CXCR4 in a variant of the pEYFP-N1 plasmid **(B)** Fluorescence microscopy images of PANC-1 CXCR4-EYFP and MIA PaCa-2 CXCR4-EYFP cells. Blue-DAPI, yellow-EYFP. Flow cytometry plots obtained during the analysis of CXCR4-EYFP⁺ cells in PANC-1 CXCR4-EYFP and MIA PaCa-2 CXCR4-EYFP cell lines. Parental cells were used as control for gating purposes.

3.4. CXCR4-EYFP PDAC cell lines secrete CXCR4-EYFP⁺ exosomes

In order to validate the expression of CXCR4-EYFP in our clones, western-blots were performed in MIA PaCa-2 CXCR4-EYFP and PANC-1 CXCR4-EYFP cells (**Figure 7A**). Additionally, to ensure that both cell lines expressed the CXCR4-EYFP fusion protein and not only the CXCR4 protein and/or EYFP protein alone we performed western blots for both GFP, which allows the detection of the EYFP protein due to significant similarity, and CXCR4. Independently of using an anti-GFP or anti-CXCR4 antibody we detected a specific band present at the expected molecular weight for the fusion protein (67 kDa) in both cell lines (**Figure 7A**). As expected, PANC-1 CXCR4-EYFP cell line expressed more CXCR4-EYFP when compared with MIA PaCa-2 due to the cell line enrichment (**Figure 7A**).

Moreover, because our goal was to generate color-coded CXCR4⁺ exosomes in order to assess their biodistribution *in vivo*, we analysed the presence of CXCR4-EYFP in exosomes derived from MIA PaCa-2 CXCR4-EYFP and PANC-1 CXCR4-EYFP cell lines by western-blot (**Figure 7B**). Western-blots using anti-GFP and anti-CXCR4 antibodies were performed in order to show signal specificity and CXCR4-EYFP fusion protein integrity. According to our results, both cell lines secrete exosomes that harbor CXCR4-EYFP fusion protein (**Figure 7B**). Additionally, exosomes derived from PANC-1 CXCR4-EYFP cells have higher levels of the fusion proteins than the exosomes derived from MIA PaCa-2 CXCR4-EYFP cells (**Figure 7B**). Interestingly, in exosomes we are able to identify two CXCR4-EYFP specific bands. One of the bands has the expected molecular weight for the fusion protein (67 kDa) while the other has a higher molecular weight.



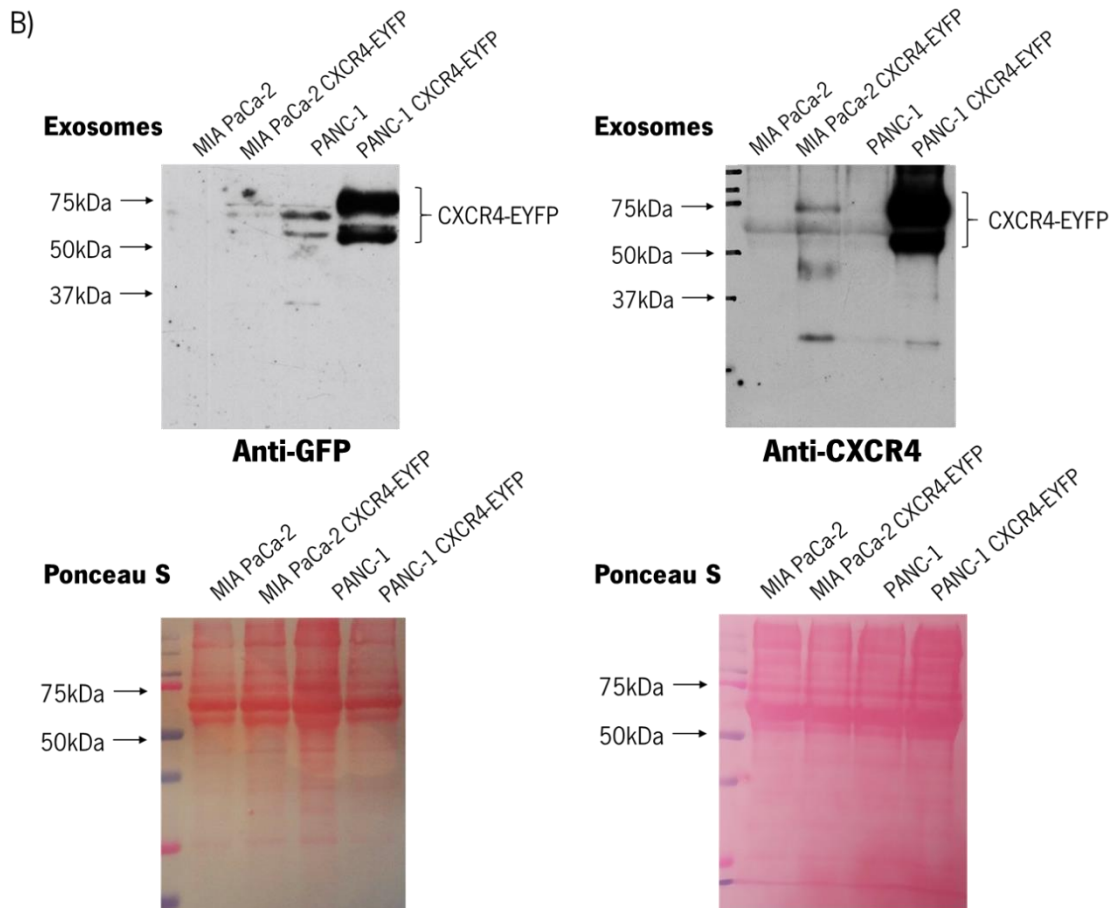


Figure 7. CXCR4-EYFP PDAC cell lines secrete CXCR4-EYFP+ exosomes. (A) Western blot analysis of CXCR4-EYFP in MIA PaCa-2, MIA PaCa-2 CXCR4-EYFP, PANC-1 and PANC-1 CXCR4-EYFP cells. Left - anti-GFP, right – anti-CXCR4. β -actin was used as loading control. (B) Levels of CXCR4 and CXCR4-EYFP in MIA PaCa-2, MIA PaCa-2 CXCR4-EYFP, PANC-1 and PANC-1 CXCR4-EYFP derived-exosomes. Exosomes extracts were separated by SDS-PAGE and analysed by western blotting. On the left, anti-GFP antibody was used. On the right, anti-CXCR4 antibody was used. Ponceau staining was used as loading control. (B) Western blot analysis of CXCR4-EYFP in MIA PaCa-2, MIA PaCa-2 CXCR4-EYFP, PANC-1 and PANC-1 CXCR4-EYFP derived exosomes. Exosomes extracts were separated by SDS-PAGE and analysed by western blotting. Left - anti-GFP, right – anti-CXCR4. Ponceau staining was used as loading control.

This might indicate the presence of two isoforms of CXCR4-EYFP in exosomes, a fact previously described in cells (Lapham et al., 2002). Due to the greater amount of CXCR4-EYFP present in the PANC-1 CXCR4-EYFP-derived exosomes, we used only the PANC-1 CXCR4-EYFP cell line on the following experiments.

Therefore, we could demonstrate that pancreatic cancer cell lines that express CXCR4-EYFP fusion protein secrete exosomes that carry that same protein.

3.5. CXCR4-EYFP exosomes flow between cancer cells

After confirming that exosomes secreted by PANC-1 CXCR4-EYFP cells harbor the fusion protein (**Figure 8A**), we wanted to assess if we were able to visualize fluorescently-labelled exosomes by imaging techniques. Therefore, we performed a co-culture between PANC-1 CXCR4-EYFP and PANC-1 CD81-Tomato cells. PANC-1 CD81-Tomato cell line, previously developed and validated in the lab, expresses a known exosomal marker (CD81) fused with a fluorescent protein (Tomato) and in this way this cell secretes CD81-Tomato color-coded exosomes. Upon co-culture we have tracked fluorescently labelled exosomes exchange between cells using advanced confocal microscopy (**Figure 8B**). As observed by confocal microscopy, both PANC-1 CXCR4-EYFP and PANC-1 CD81-Tomato cells secrete fluorescently-labelled exosomes that correspond to the small yellow and red dots (**Figure 8B**, please refer to the arrows). Additionally, we could observe a flow of CXCR4-EYFP positive exosomes from the producing cells (PANC-1 CXCR4-EYFP) to the recipient cells (PANC-1 CD81-Tomato; **Figure 8B**). These results confirm that PANC-1 CXCR4-EYFP-derived exosomes are fluorescently labelled, and we are able to visualize them by imaging techniques, ultimately, validating our model. Most importantly, we could demonstrate that CXCR4-EYFP exosomes are exchanged between different cancer cells.

3.6. PANC-1 CXCR4-EYFP+ exosomes accumulate more in CXCL12-embedded plugs

We orthotopically injected PANC-1 CXCR4-EYFP cancer cells in the pancreas of Rag2^{-/-}; IL2rg^{-/-} immunodeficient mice. Mice developed pancreatic tumors with 100% penetrance (**Figure 10A**). After the tumors reached 1000mm³ size in average, mice were inoculated with two Matrigel plugs, placed in the back of the animal, equidistant to the pancreas (**Figure 9A**). One of the Matrigel plugs in each mouse was used as control (H₂O), and the second plug was embedded in recombinant CXCL12. Mice were randomized in different treatment groups: GW4869, a drug previously used and validated to inhibit exosomes secretion (Essandoh et al., 2015). In this group we were aiming to inhibit secretion of cancer exosomes; neutralizing anti-CXCR4 rabbit antibody was used to treat animals and inhibit CXCR4 present in cancer cells but also cancer exosomes; control groups were DMSO (GW4869 vehicle) and rabbit IgG treated (anti-CXCR4 control). Treatments started in the groups one day before the plugs inoculation.

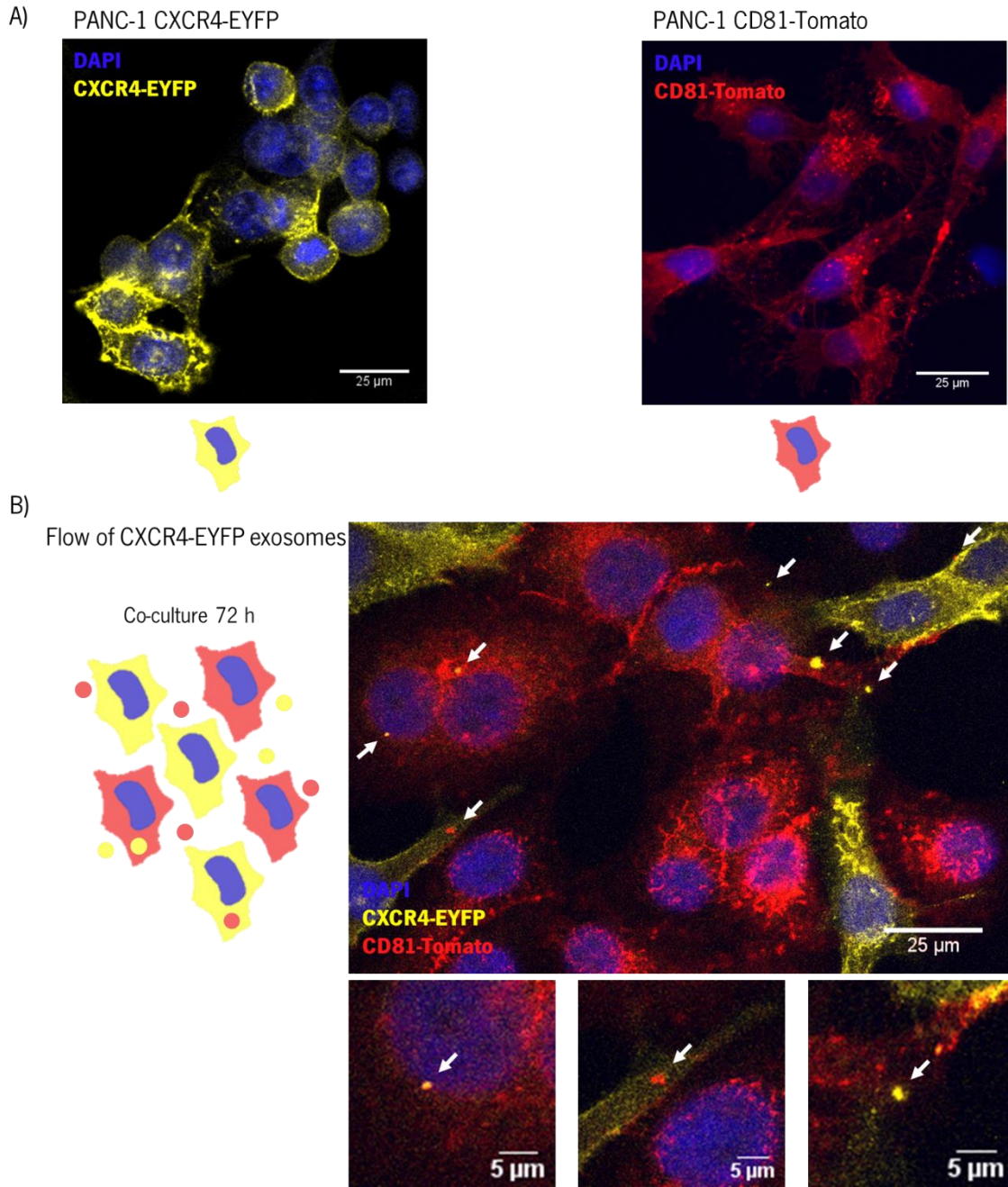


Figure 8. CXCR4-EYFP exosomes flow between cancer cells. (A) Confocal microscopy images of PANC-1 CXCR4-EYFP and PANC-1 CD81-Tomato cells. Blue – DAPI, Yellow- CXCR4-EYFP, Red – CD81-Tomato **(B)** Flowchart of PANC-1 CXCR4-EYFP and PANC-1 CD81-Tomato co-culture. Confocal microscopy images of PANC-1 CXCR4-EYFP and PANC-1 CD81-Tomato co-culture. Blue – DAPI, Yellow- CXCR4-EYFP, Red – CD81-Tomato. Arrows – exosomes

Prior to mice euthanasia after the 5 days of treatment, Matrigel plugs were carefully removed **(Figure 9A)**. In some animals from the different groups, plugs were not found or were degraded reducing the number of animals per group. Representative images of IVIS Spectrum CT In Vivo Imaging System fluorescence quantification of control and rCXCL12 plugs from the different groups

were taken (**Figure 9A**). Upon evaluation of total fluorescence of control and rCXCL12 plugs independent of the treatment group, we observe a tendency to an increased accumulation of CXCR4-EYFP⁺ exosomes (1,16-fold change) in rCXCL12 plugs when compared with the control (**Figure 9B**). This result demonstrates a possible role for CXCR4 in exosomes biodistribution tightly associated with CXCL12 presence.

Additionally, analysis of the fold-change of the maximum intensity between the rCXCL12 plug and the control plug for each animal was calculated. Fluorescence ratios were 1.2 in IgG treated group, 1.2 in anti-CXCR4 treated group, 1.4 in DMSO treated group and 0.9 in GW4869 treated group (**Figure 9B**). Overall, this result demonstrates that in the majority of the animals the rCXCL12 plug had higher fluorescence values than the control plug, demonstrating once again that CXCR4-EYFP⁺ exosomes tend to accumulate more where CXCL12 is present (**Figure 9B**). When comparing the IgG treated group CXCL12/control plugs fluorescence ratio with the anti-CXCR4 treated group no statistical significant differences were found (**Figure 9B**). This can indicate that the concentration used of neutralizing antibody, despite being described as having an effect on CXCR4-mediated processes in cells, could not be sufficient to affect CXCR4-mediated processes in exosomes. Additionally, the difference of plugs fluorescence ratio between the DMSO treated and the GW4869 treated group was not statistically significant (**Figure 9B**). However, it is possible to see a clear downward trend in the GW4869 treated group when compared with control (**Figure 9B**).

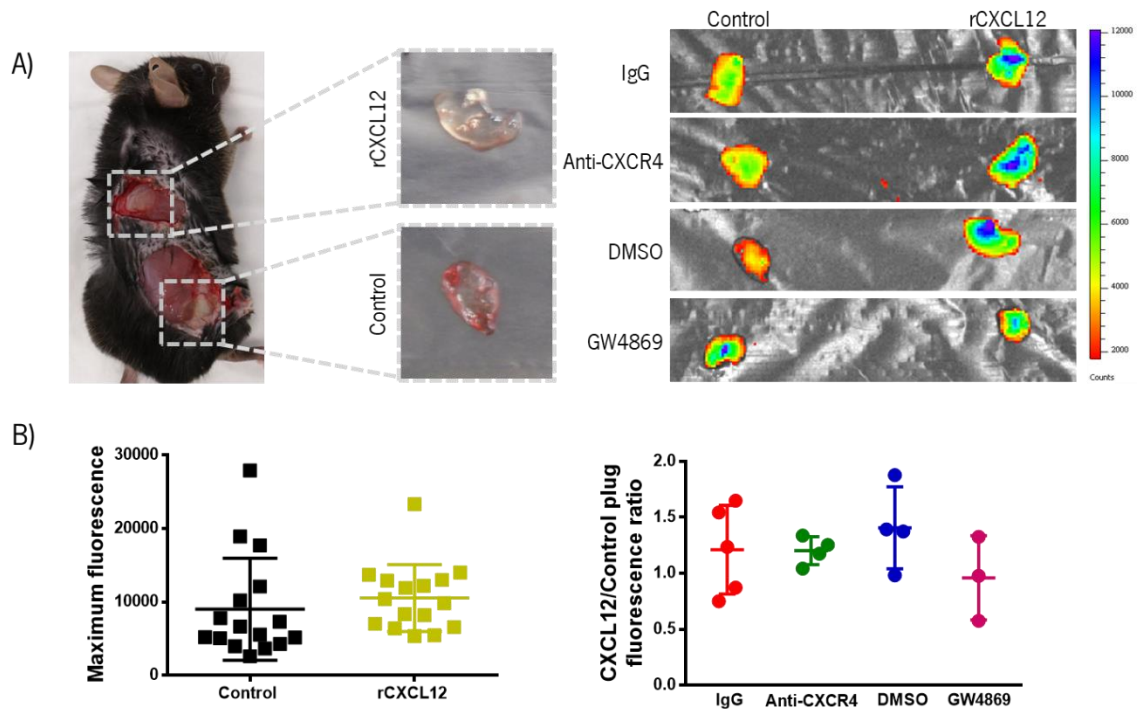
Plugs were also analysed by confocal microscopy (**Figure 9C**). Using the ImageJ program, the mean intensity of fluorescence was measured considering the plug area and the fold-change between the rCXCL12 plug and the control plug was calculated (**Figure 9C**). All plugs had background fluorescence that was not specific. To quantify cells or exosomes-specific fluorescence the settings of Brightness/Contrast were adjusted to reduce the background fluorescence (minimum=20, maximum=255). Upon DAPI staining analysis we could observe that the fluorescence does not co-localize in its entirety with the marked nuclei showing that the EYFP signal is not cell-related (**Figure 9C**).

Plugs fluorescence ratio between the rCXCL12 plug and the control plug is 1.5 IgG treated group, 1.2 in anti-CXCR4 treated group, 1.4 in DMSO treated group and 1.3 in GW4869 treated group (**Figure 9C**). The values of plugs fluorescence ratios in the different treatment groups obtained with the ImageJ analysis despite not fully matching IVIS analysis demonstrate the same

trend of CXCR4-EYFP⁺ exosomes accumulating more in rCXCL12 plugs than the control plugs. The variations observed in the plugs fluorescence ratios between the anti-CXCR4 treated group and respective control as well as the GW4869 treated group and respective control present the same trends as in the IVIS analysis confirming the results obtained previously.

H&E analysis demonstrated the presence of the tumors in the pancreas (**Figure 10A**), and confocal microscopy analysis allowed to confirm the presence of PANC-1 CXCR4-EYFP-derived tumors through the observation of the EYFP signal (**Figure 10A**). Among the different groups, there were no significant differences in tumor weight and volume of the pancreas (**Figure 10B**). The number of liver macro-metastasis are not statistically significant different between the different groups (**Figure 10B**).

These results confirm that the different animals were correctly randomized between the different groups. The number of exosomes present in circulation was not statistical significant between the different groups (**Figure 10C**). In this case, although the differences are not statistically significant there is a tendency for an increase in the number of exosomes in the anti-CXCR4-treated group as compared to the IgG-treated group (**Figure 10C**). When comparing the DMSO-treated group to the GW4869-treated group, we see that there is also a tendency for a reduction in the number of exosomes in the GW4869-treated group (**Figure 10C**).



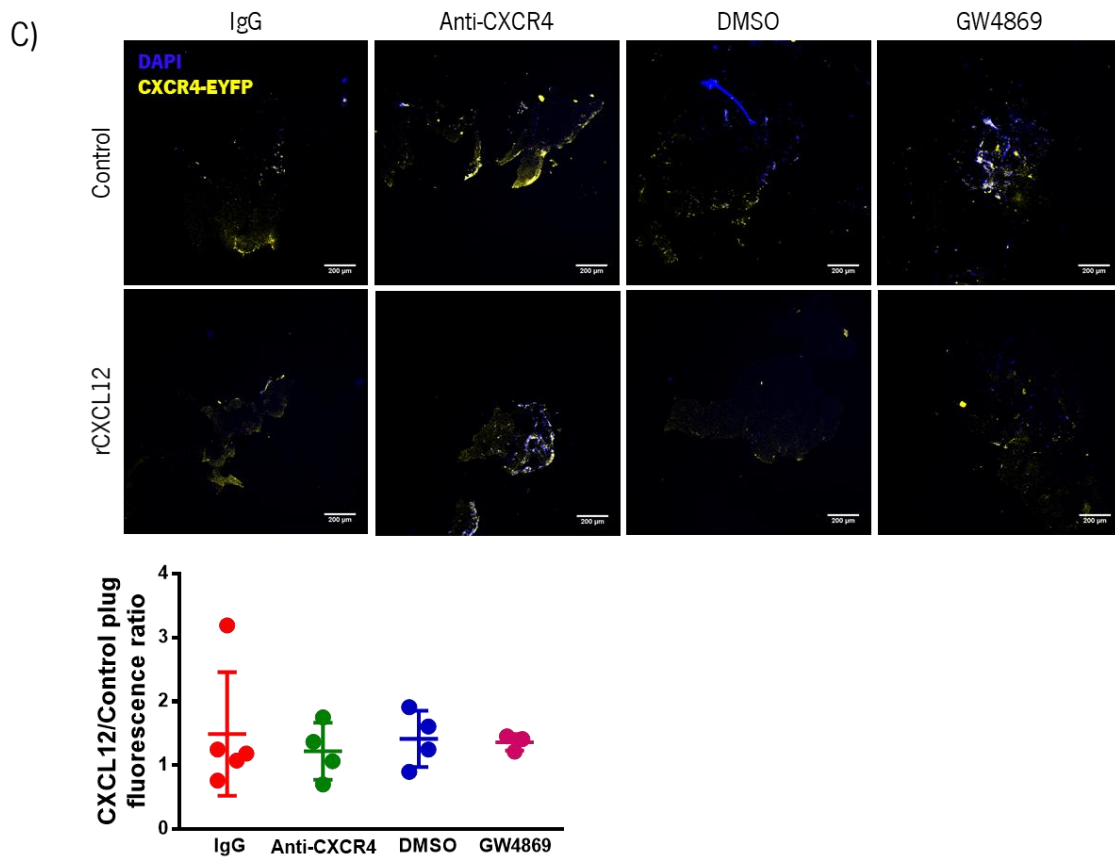


Figure 9. PANC-1 CXCR4-EYFP⁺ exosomes accumulate more in CXCL12-embedded plugs. (A)

Representative image of rCXCL12 and control plugs localization in mice back. Representative images of rCXCL12 and control plugs after removal from mice back. Representative fluorescence image of rCXCL12 and control plugs for the different treatment groups measured using the IVIS Spectrum CT In Vivo Imaging System. Fluorescence intensity: Red - Minimum, Blue - Maximum. **(B)** Maximum fluorescence intensity measured using IVIS Spectrum CT In Vivo Imaging System in rCXCL12 and control plugs of all mice independently of the treatment group. rCXCL12/control plugs maximum fluorescence ratio in IgG-treated, CXCR4 neutralizing antibody-treated, DMSO-treated and GW4869-treated mice groups. Plugs maximum fluorescence was measured using IVIS Spectrum CT In Vivo Imaging System **(C)** Representative confocal images of rCXCL12 and control plugs from the IgG-treated, CXCR4 neutralizing antibody-treated, DMSO-treated and GW4869-treated mice groups. Blue - DAPI, Yellow - CXCR4-EYFP. rCXCL12/control plugs mean fluorescence intensity per plug area ratio in IgG-treated, CXCR4 neutralizing antibody-treated, DMSO-treated and GW4869-treated mice groups. Plugs mean fluorescence intensity per plug area ratio was measured using Fiji (ImageJ) software. Scale bar = 200 μ m. Data shown as mean \pm SD. Statistical significance was determined using Kruskal-Wallis Test.

Concerning the presence of CXCR4-EYFP in the exosomes present in circulation, we observe that the majority of exosomes in circulation are CXCR4-EYFP⁺ (**Figure 10D**). Although there are no differences between the different experimental groups, this proves that PANC-1 CXCR4-EYFP cells are able to secrete CXCR4-EYFP⁺ into circulation and this constitutes the majority of exosomes in the bloodstream (**Figure 10D**).

3.7. CXCR4⁺ exosomes are not enriched in the serum of KPC mice with higher frequency of metastasis

KPC is a genetically engineered mouse model of pancreatic cancer that histologically reflects the human disease (Westphalen & Olive, 2012b). These animals have a heterozygous Kras^{G12D} mutation, and an heterozygous TP53^{R172H} mutation, under the Pdx-1 pancreas-specific promoter (Kras^{G12D}^{+/+}; TP53^{R172H}^{+/+}; Pdx-1^{Cre/+}), and spontaneously develop pancreatic ductal adenocarcinoma that progresses as the human disease. We used these animals to address the enrichment of CXCR4⁺ exosomes in circulation, and to understand if this amount was somehow correlated with number of metastasis in this mouse model.

KPC mice were euthanized at 27 weeks of age (**Figure 11A**). At this age these animals usually have already developed a pancreatic tumor mass and macrometastasis in the liver and/or lung. At the time of euthanasia, blood was collected, and serum isolated to quantify the number of exosomes in circulation and to evaluate the presence of CXCR4 in serum exosomes. Comparing the number of exosomes between the different animals we observe that the animal 1037 was the one with slightly more exosomes while the animal 1397 was the one with the lower number of exosomes (**Figure 11B**). The other animals had similar levels of serum exosomes (**Figure 11B**). Concerning the presence of CXCR4 in the serum exosomes, flow cytometry analysis indicated that all animals had exosomes containing the protein of interest (**Figure 11B**). CXCR4 protein levels remained very constant in 4 of the 5 animals analysed, with levels close to 0.4% (**Figure 11B**). Interestingly, animal 851 had CXCR4 levels above 1% (**Figure 11B**).

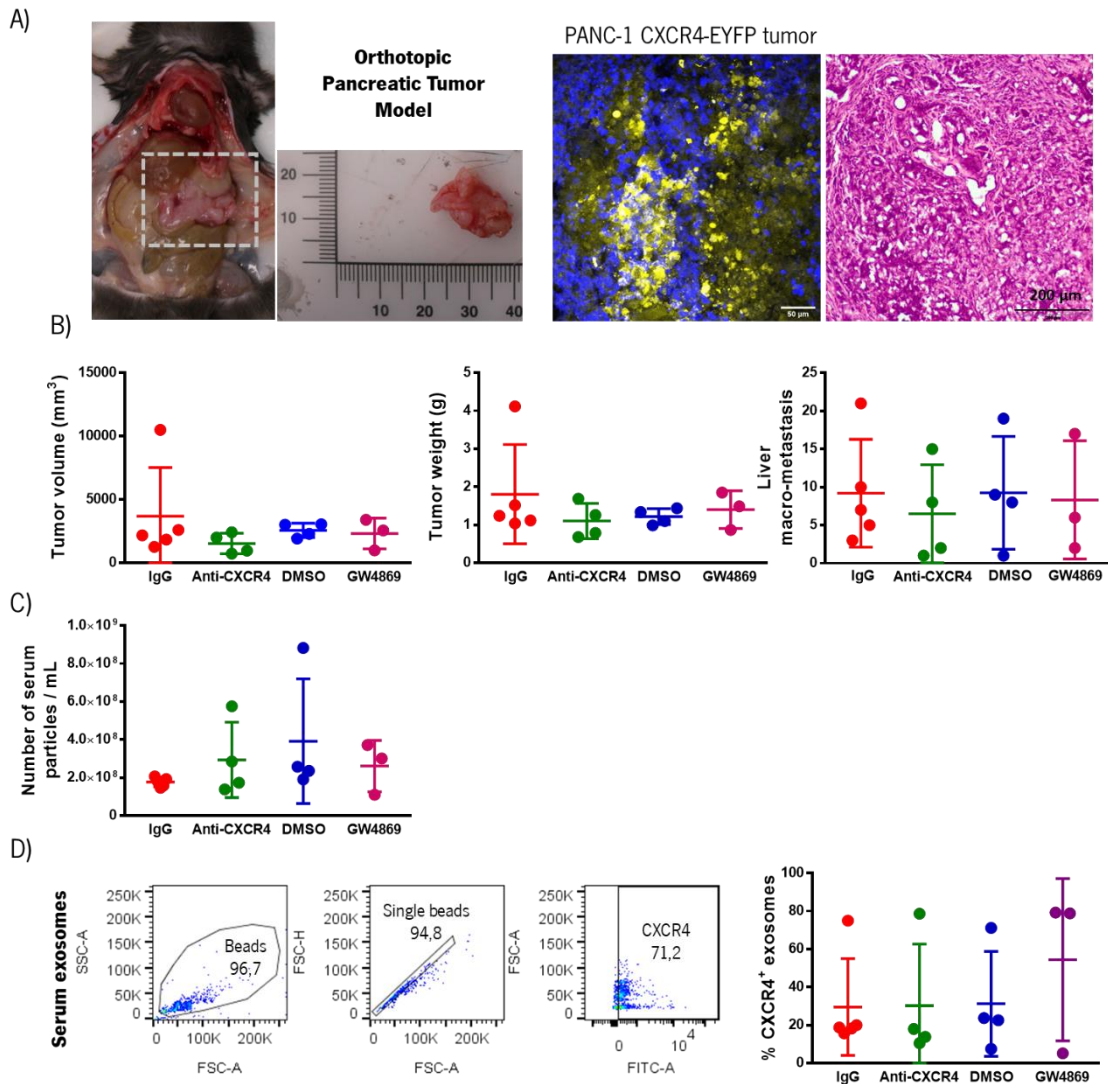
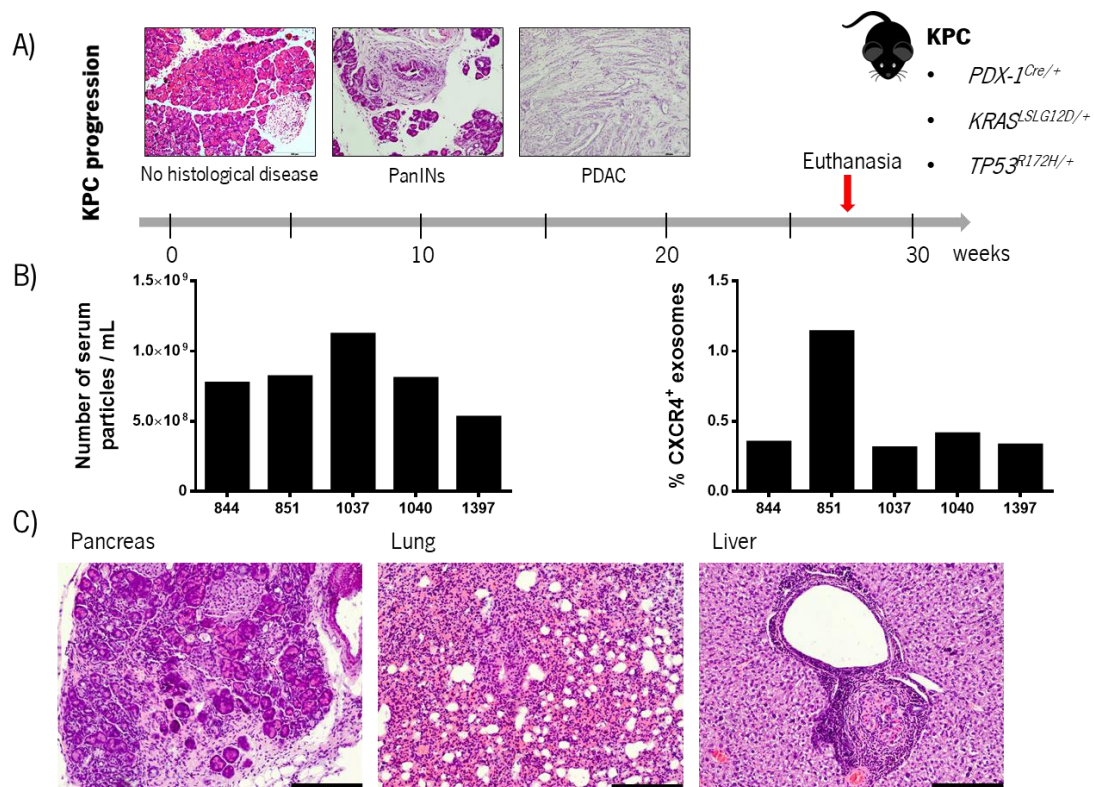


Figure 10. CXCR4-EYFP⁺ exosomes are present in the bloodstream. (A) Representative PANC-1 CXCR4-EYFP tumor image. Representative confocal image of a PANC-1 CXCR4-EYFP tumor. Blue – DAPI, Yellow – CXCR4-EYFP. Scale bar = 50 μm . H&E image of a PANC-1 CXCR4-EYFP tumor. Scale bar = 200 μm . **(B)** Tumor volume (mm^3), tumor weight (g) and number of liver macro-metastasis of the IgG-treated, CXCR4 neutralizing antibody-treated, DMSO-treated and GW4869-treated mice groups. **(C)** Number of serum exosomes at the time of euthanasia of the IgG-treated, CXCR4 neutralizing antibody-treated, DMSO-treated and GW4869-treated mice groups. **(D)** Representative serum CXCR4⁺ exosomes flow cytometry plots. Percentages of serum CXCR4⁺ exosomes in the IgG-treated, CXCR4 neutralizing antibody-treated, DMSO-treated and GW4869-treated mice groups. Exosomes stained with secondary antibody only were used as controls. Data shown as mean \pm SD. Statistical significance was determined using Kruskal-Wallis Test.

However, the increase in the number of CXCR4⁺ exosomes in animal 851 is not justified by a greater presence of PDAC cells. Upon histopathological analysis, supported by experts in the lab, we observed that the animal 844 had 20% PanIN lesions and 80% of PDAC; animal 851 had 70% "normal" tissue and 30% PDAC; animals 1037 and 1397 had 95% "normal" tissue and 5% PDAC; animal 1040 had 85% "normal" tissue and 15% PDAC (**Figure 11C**). Apparently, no animal had lesions in the lung. Concerning the liver lesions, only the animals 844 and 1397 had macrometastasis (**Figure 11C**). Representative H&E images of "normal" tissue, PanIN lesions (histologically well-defined precursor lesions to PDAC) and PDAC are present in (**Figure 11C**). CXCR4 expression was analysed in PDAC and liver tissue sections of the KPC mice by immunohistochemistry to observe if there was a correlation between CXCR4⁺ tumor cells and the number of CXCR4⁺ exosomes in the serum. The number of CXCR4⁺ tumor cells were very low in three out of five KPC mice (851, 1040 and 1397) and not present in two out five animals (844 and 1037; **Figure 11D**). Regarding the CXCR4 expression in the liver we did not see any specific staining in both the metastatic lesion and the normal tissue (**Figure 11D**).

With these results there was no evident correlation between the presence of macrometastasis and CXCR4 positive exosomes in circulation. An increase in the number of animals as well as the assessment of micrometastasis could provide stronger data assessment.



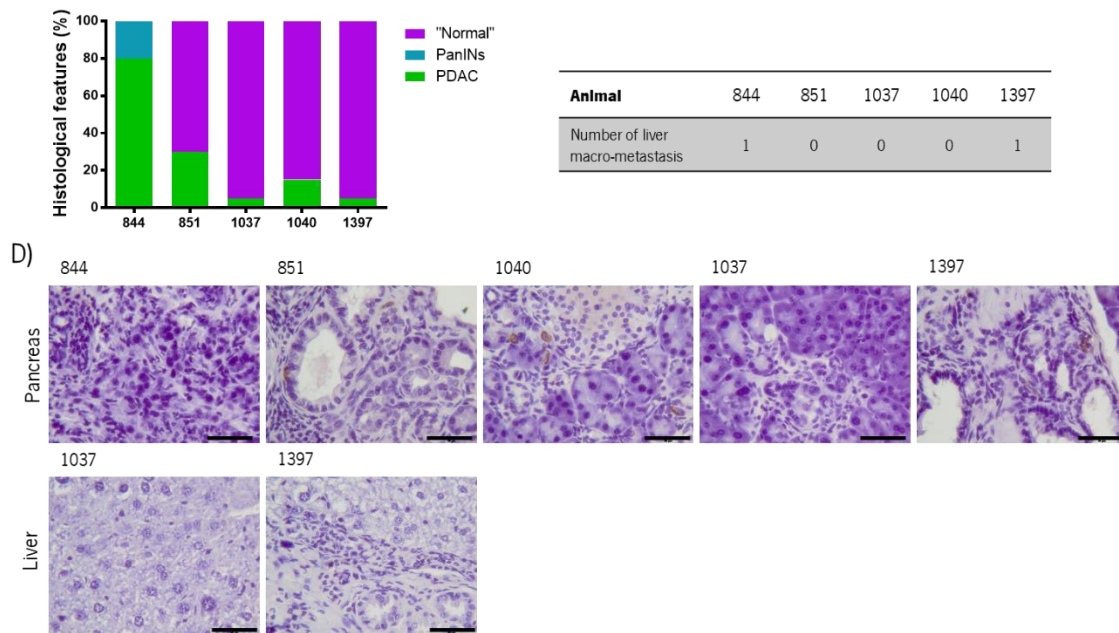


Figure 11. CXCR4⁺ exosomes are not enriched in the serum of KPC mice with higher frequency of metastasis. (A) Schematic representation of KPC (Kras^{G12D^{+/+}}; TP53^{R172H^{+/+}}; Pdx-1^{Cre/+}) progression timeline with representative H&E images of the different stages of disease progression. Red arrow – Day of euthanasia. (B) Total number of serum exosomes and percentage of serum CXCR4⁺ exosomes at the time of euthanasia of the different KPC mice. Exosomes stained with secondary antibody only were used as controls. n=1. (C) Representative H&E images of the pancreas, lung and liver of the KPC mice. Scale bar= 200 μ m. Histopathological score of the KPC mice pancreas in three categories: “Normal” = No histological disease; PanINs =Pancreatic Intraepithelial Neoplasia and PDAC = Pancreatic Ductal Adenocarcinoma. Percentages were determined by an expert using a representative H&E of the KPC mice pancreas. Table with the number of liver macro-metastasis at the time of euthanasia in the KPC mice. (D) Representative CXCR4 IHC images of the primary tumor and liver of the KPC mice. CXCR4 staining in normal liver tissue (1037) and in a liver metastatic lesion (1397) are present. Scale bar= 50 μ m.

4.DISCUSSION

Exosomes are a subclass of extracellular vesicles released by several types of cells that play a critical biological role in intercellular communication. They are involved in a broad variety of cellular processes in health and disease. In cancer, exosomes appear to mediate the interaction between cancer cells and their microenvironment and play a critical role in cancer development. It has been described that tumor cells produce and secrete more exosomes than normal cells. Recent discoveries revealed that cancer cells release soluble factors that modulate distant organs microenvironment supporting the metastatic process (Peinado et al., 2017). Exosomes are one of these tumor-derived factors and the formation of pre-metastatic niches appears to be dependent on tumor-derived exosomes (Hood, San, & Wickline, 2011; Peinado et al., 2012). Exosomes are present in the circulation and have access to all parts of the body, representing a form of communication between cells. It has been demonstrated that cancer exosomes are able to recapitulate the organ specificity of their cell of origin due to the presence of surface components.

Despite this, the mechanism that determines the fate of exosomes to specific metastatic sites is not fully understood. The chemokine receptor CXCR4 appears to be the most common chemokine receptor expressed in most types of cancer cells. In PDAC, CXCR4 is expressed in a subpopulation of migrating pancreatic cancer stem cells that appears to be involved in tumor metastasis. We observed that PANC-1 and MIA PaCa-2 cell lines have both very low levels of CXCR4 at their membrane never exceeding 6%. Moreover, since it is described that a subpopulation of CXCR4⁺CD133⁺ pancreatic cancer cells could be pancreatic cancer stem cells, we evaluated the co-expression of these two molecules in PANC-1 and MIA PaCa-2 cells. Results showed that in MIA PaCa-2 cells around 90% of CXCR4 positive cells were positive for CD133, while in PANC-1 cells only 70% of CXCR4 positive cells had positive staining for CD133. These results are in accordance with the literature and validate that the cell lines selected to perform this study allow the study of the role of CXCR4 in PDAC progression.

Additionally, CXCR4 is a membrane receptor that is actively internalized, being also present in the cytoplasm. Taken this into account, we investigated the intracellular expression of CXCR4 in permeabilized PANC-1 and MIA PaCa-2 cells. The results showed that intracellular levels of CXCR4 were almost 100% in both cell lines indicating that CXCR4 was mostly present in internal compartments. After internalization, the CXCR4 receptor can be recycled back to the plasma membrane or it can be ubiquitinated and sorted to the lysosome for further degradation (Orsini, Parent, Mundell, & Benovic, 1999) (Marchese, Chen, Kim, & Benovic, 2003). Several studies suggest that the fate of the receptor after internalization may be dictated by modifications that

occur on specific residues (Busillo & Benovic, 2007). Studies have shown that CXCR4 is most likely ubiquitinated on one of three lysines residues (Lys327, Lys331, or Lys333) in the C-terminal tail. Mutation of these three residues to arginine eliminates ubiquitination and degradation of the receptor (Marchese & Benovic, 2001). Our results suggest that in our cell lines the CXCR4 receptor is not being expressed at the cell membrane of the cells but instead is being accumulated in the cytoplasm. Studies regarding the localization of CXCR4 in hematopoietic progenitor cells demonstrated that the surface expression of the receptor is low, whereas a large part of the protein is sequestered intracellularly (Cepeda et al., 2015; Zhang et al., 2004). They found that most of the CXCR4 is in endomembranes colocalizing with markers of the Golgi apparatus and early and recycling endosomes (Zhang et al., 2004). These intracellular vesicular deposits presented a perinuclear pattern of subcellular localization (Cepeda et al., 2015). Interestingly, it has been described that membrane CXCR4 undergoes an internalization process through a clathrin-mediated endocytic pathway (Signoret et al., 1997) (Zhang et al., 2004). During exosomes biogenesis, the inward budding of clathrin-coated domains in the plasma membrane leads to the formation of intraluminal vesicles (ILVs) that can then be released to the extracellular space being then defined as exosomes (Colombo et al., 2014). The mechanism that leads to the CXCR4 internalization and the first steps of exosomes biogenesis is common. This suggests that after CXCR4 internalization, this receptor can be sorted into intraluminal vesicles (ILVs). Upon ILVs accumulation in the endosomal lumen, the endosomes become multivesicular bodies (MVBs) that can persist in the cytosol for variable periods of time. MVBs can then undergo exocytic fusion with the plasma membrane releasing the ILVs (now defined as exosomes) to the extracellular space. Taken this together, we decided to evaluate if CXCR4 was being shuttled to exosomes membrane and if it could be associated with any exosomes-associated process.

Evaluation of CXCR4 presence in exosomes membrane by flow cytometry in the cell lines in study showed that similar to what we observed in the parental cells, the levels of CXCR4 in MIA PaCa-2 and PANC-1 derived exosomes were very low, never exceeding 2%. Although the differences were not statistically significant, MIA PaCa-2 derived exosomes presented a slight increase in the levels of CXCR4 when compared with PANC-1 derived exosomes. Since the majority of pancreatic cancer cells that present CXCR4 in their cell membrane also present CD133, we analysed the presence of CD133 in the CXCR4⁺ exosomes. Flow cytometry results demonstrate that both MiaPaca-2 CXCR4⁺ exosomes and PANC-1 CXCR4⁺ exosomes have CD133 in their membranes with similar percentages. 25% of the PANC-1 CXCR4⁺ exosomes were also positive for CD133 and 30%

of MiaPaca-2 CXCR4⁺ exosomes were positive for CD133. Regarding the levels of co-expression of CXCR4 and CD133 in pancreatic cancer cells we observed that the levels of co-expression of these markers found in exosomes was lower. So far, it is still not possible to perform flow cytometry analysis of single exosomes due to their small size. The only way to perform this experiment is to analyse latex beads coupled with exosomes. This way, when performing exosomes flow cytometry analysis, we are not analysing single exosomes, but instead, we are analysing single beads with exosomes attached to it. There is no way to control or to know how many exosomes bind to a single bead. During the analysis we are not doing a 1:1 comparison as in cells, which can interfere with the obtained results. CD133 is a cancer stem cell marker and is normally present at low levels and taking in consideration our results we demonstrate that cells are able to sort this protein into exosomes. There are no reports so far in the literature about the presence of CD133 in pancreatic cancer exosomes neither their biological significance *in vivo*. Further studies are needed to understand the role of CD133 protein in exosomes and evaluate if it could be associated with the role of exosomal CXCR4.

Exosomal integrins have been described as mediators of exosomes organotropism aiding exosomes fusion with specific cells at distant sites (Hoshino et al., 2015). Taking this in consideration and followed by our results, we hypothesised that the presence of CXCR4 in cancer exosomes could facilitate their retention at CXCL12-enriched organs and, ultimately, lead to modulation of cells present at these distant sites. To test our hypothesis, MIA PaCa-2 and PANC-1 cells were transiently transfected with a plasmid containing the C-terminal end of the rat CXCR4 fused with the yellow (EYFP) version of the green fluorescent protein. This will allow the *in vitro* and *in vivo* tracking of both cells and exosomes. The percentage of CXCR4-EYFP⁺ cells in PANC-1 CXCR4-EYFP clone was around 95%, indicating a stable clone. Unfortunately, the percentage of CXCR4-EYFP⁺ cells in MIA PaCa-2 CXCR4-EYFP never exceeded 50%. This result could indicate that the fusion protein is leading to cell growth disadvantage or to cell death. Since our main goal with this work was to study the role of CXCR4⁺ exosomes in PDAC progression and generate tools that allowed us to track exosomes *in vivo* and *in vitro* we decided not to pursue further this result.

The images obtained through fluorescence microscopy corroborate the flow cytometry analysis. Despite this, the fusion protein CXCR4-EYFP has a cell distribution that mimics endogenous CXCR4 because it is localized mainly in the plasma membrane, but it is also present in the cytoplasm being visible perinuclear localization. The presence of CXCR4-EYFP in the cytoplasm indicates that

the fusion protein is being recycled and can follow the same endocytic pathway as endogenous CXCR4 which can lead to it being shuttled into exosomes.

To further validate that the fusion protein is being correctly expressed in MIA PaCa-2 CXCR4-EYFP and PANC-1 CXCR4-EYFP, we analysed by western blot CXCR4-EYFP in both cell lines. To confirm that the cell lines in study express the fused protein CXCR4-EYFP and not only the CXCR4 protein and/or EYFP protein alone we performed a western blot using an anti-GFP antibody, that allows the detection of EYFP due to the aminoacid sequence overlap, and another using an anti-CXCR4 antibody. CXCR4 has a predicted 40 kDa molecular weight while EYFP has a predicted 27 kDa molecular weight. This way the fusion protein must have a molecular weight of around 67 kDa. The results show that in both clones and regardless of the antibody used it is detected a band with the molecular weight expected for the fusion protein. This band is not detected in the parental cell lines confirming that both clones express the fusion protein. The band from the PANC-1 CXCR4-EYFP cells is more intense when compared with the band from MIA PaCa-2 CXCR4-EYFP cell suggesting that the PANC-1 clone expresses more CXCR4-EYFP protein. These results were expected because the flow cytometry results showed that the CXCR4-EYFP⁺ cells in MIA PaCa-2 CXCR4-EYFP were only around 50% while in PANC-1 CXCR4-EYFP was over 90%. The same analysis was performed for exosomes derived from the cell lines in study. Analysing both western blots, we observe that CXCR4-EYFP fusion protein is mainly present in the PANC-1 CXCR4-EYFP cell line. Additionally, in the anti-GFP and anti-CXCR4 western-blots two specific bands are detected in the PANC-1 CXCR4-EYFP derived exosomes. One of the bands corresponds to the expected size of the fusion protein while the other has a higher size. The higher size band can correspond to post-translational modifications that occurred in the fusion protein that can facilitate CXCR4-EYFP shuttling to exosomes. Ultimately, since the fusion protein is almost not present in MIA PaCa-2 CXCR4-EYFP derived exosomes we did not use this cell line for further experiments.

Furthermore, the 72h co-culture performed between the PANC1 CXCR4-EYFP and the PANC1 CD81-Tomato further confirmed that the PANC-1 CXCR4-EYFP cell line secreted fluorescently-labelled exosomes and that these exosomes are able to be taken up by other cells.

After validating the tools developed to track CXCR4⁺ exosomes *in vivo*, PANC-1 CXCR4-EYFP cells were orthotopically injected in immunodeficient mice. Tumors were allowed to grow until they reached the volume equivalent to or greater than 1000 mm³ to then perform the Matrigel plugs experiment and evaluate the biodistribution of CXCR4-EYFP exosomes. A total of 22 animals was

used for the experiment. Twenty animals were implanted with the rCXCL12 and control plugs and two animals were used as controls. The purpose of performing an experiment using plugs was to recreate an organ that produced high levels of the chemokine CXCL12 which is the receptor ligand for the CXCR4 receptor, rCXCL12 plug, and one that does not, the control plug. The 20 animals were divided into 4 experimental groups with 5 animals per group: IgG treated, neutralizing CXCR4 antibody treated, DMSO treated and GW4869 treated. A short period after surgery two animals were found dead due to unknown causes since no tumor was detected, reducing the number of animals for the experiment. Before mice euthanasia, the Matrigel plugs were carefully removed from the animals. Regarding our hypothesis, we would expect that CXCR4-EYFP⁺ exosomes would be retained in greater extent in the plug containing the respective ligand (rCXCL12) compared to the control plug. The higher amount of CXCR4-EYFP⁺ exosomes would contribute to a greater amount of fluorescence throughout the plug when compared with the control. Using the IVIS Spectrum CT In Vivo Imaging System fluorescence intensity was measured. After quantification, the ratio of the maximum intensity between the rCXCL12 plug and the control plug was calculated. The measurement of the maximum fluorescence intensity demonstrated that independently of the treatment group there is a higher mean fluorescence intensity in the rCXCL12 plugs than the control plugs. Despite IVIS quantification allowing the most representative measurement of the fluorescence intensity of all the plug, this type of analysis does not allow to control the possibility of the fluorescence being cell-derived and not exosomes-derived. Thus, we can not conclude with certainty that more CXCR4-EYFP exosomes are retained in the rCXCL12 plugs. Additionally, we compared the rCXCL12/control plugs fluorescence ratios between the different treatment groups. The mean plugs fluorescence ratio in IgG group was around 1.2 meaning that the maximum intensity of fluorescence of the plugs with rCXCL12 was higher than the control group (ratio>1). The same result was obtained in the CXCR4 neutralizing antibody group. Thus, no significant differences were detected between the neutralizing anti-CXCR4 group and the respective control. Since the CXCR4 neutralizing antibody would bind to the CXCR4-EYFP in exosomes, blocking the possible binding of the receptor to its respective ligand (CXCL12) would lead to loss of specificity. Ultimately, we hypothesized that the ratio of fluorescence between rCXCL12 and control plugs would decrease when compared with the control. In this experiment, the amount of neutralizing anti-CXCR4 antibody injected was based on the literature. So, since the order of magnitude of cancer exosomes compared with cancer cells is 10³ or 10⁴ greater the lack of significant differences between the two treatments might be because the insufficient amount of neutralizing CXCR4

antibody injected. An additional experiment will be performed in the future to determine the amount needed of neutralizing antibody to block CXCR4 function in exosomes.

In the DMSO treated group, the mean plugs fluorescence ratio was around 1.4, meaning that the rCXCL12 plug was more fluorescent than the control plug. In the GW4869 treated group the ratio was around 1 indicating that there were no differences in the mean fluorescence between the two plugs. The differences of the mean plugs fluorescence ratio between the DMSO and the GW4869 group were not statistically significant, however we visualize a downward trend in the GW4869 treated group. Additionally, treatment with GW4869 led to a slight reduction in the number of serum exosomes, as expected. This suggests that the number of CXCR4-EYFP⁺ exosomes in circulation was lower in the GW4869 group when compared with the DMSO group ultimately inhibiting a possible accumulation of the fluorescently labelled exosomes in the rCXCL12 plugs.

In order to confirm that the fluorescence signal observed and analysed by the IVIS system was exosomes-specific, cross-sections of the plugs stained with DAPI were analysed by confocal microscopy. Confocal microscopy analysis demonstrated that the fluorescence present does not co-localize with stained nuclei, demonstrating that exosomes fluorescence is exosomes-derived. Additionally, mean intensity of fluorescence was measured considering the plug area in order to perform a similar analysis as the one performed using the IVIS system. The results were very similar to the results obtained through IVIS quantification. The slight differences that may exist can be explained by the fact that in the IVIS analysis we are quantifying the fluorescence of the entire plug, while in this analysis we are quantifying the fluorescence of only a representative section. In this analysis only one plug section was quantified since the main goal of this analysis was to prove that the fluorescence observed through the IVIS system was exosomes-derived. Ultimately, quantification of blood vessels presence needs to be performed in order to validate that the differences observed between rCXCL12 and the control plugs are not angiogenesis-related.

H&E and confocal microscopy analysis of the mice pancreas injected with PANC-1 CXCR4-EYFP cells validated the presence of fluorescently labelled pancreatic tumors. We observe by confocal microscopy that not all cells within the tumor are CXCR4-EYFP. This result is mainly due to the high number of infiltrating cancer-associated fibroblasts, not fluorescently labelled, that characterizes pancreatic tumors and was confirmed by H&E assessment.

At the time of euthanasia, the tumor volume and tumor weight, along with a number of metastasis in liver and lung were assessed. The differences in tumor volume and weight plus the number of liver macro-metastasis between the different experimental groups were not statistically significant. Since the different treatment regimens were only performed for 6 days before euthanasia we hypothesized that the drug amount and time was not sufficient to produce significant differences.

The total number and CXCR4⁺ serum exosomes was also assessed. When comparing the DMSO treated group to the GW4869 treated group we see that there is a tendency for a reduction in the number of exosomes in the GW4869 treated group, although the differences were not statistically significant. GW4869 was already described as an inhibitor of exosomes production, ultimately leading to a reduction in exosomes release (Essandoh et al., 2015). Thus, the result obtained was as expected.

The levels of the CXCR4-EYFP⁺ exosomes present in serum exosomes were detected using the CXCR4 antibody and analysed by flow cytometry. No statistical significant results were found between the different groups. Nevertheless, a large proportion of serum exosomes were CXCR4⁺ in all animals confirming that the PANC-1 CXCR4-EYFP⁺ cells are able to secrete cancer exosomes enriched in CXCR4-EYFP into circulation. Since cancer cells secrete more exosomes than normal cells, this result was also expected (Whiteside, 2016). Ultimately, the rCXCL12 and control plugs were not present in all mice at the time of euthanasia. Therefore, these animals were removed from the analysis and the number of animals per group reduced. This experiment should be performed again with a larger number of animals to further validate our results.

The KPC mouse model is one of the GEMMs most widely used to study pancreatic cancer *in vivo* once it fully recapitulates the different stages of the human disease (Hingorani et al., 2003). We evaluated this model to determine if the levels of CXCR4⁺ serum exosomes correlated with the different stages of disease progression.

At the time of euthanasia, KPC 1037 presented the most serum exosomes when compared to the other animals. This result was not expected since, at our lab, the number of exosomes in the serum tends to correlate with an increase in tumor burden in KPC mice. Regarding the levels of CXCR4⁺ exosomes, KPC 851 presents the higher number when compared with the others. Due to CXCR4 role in PDAC progression, we hypothesized that an increase in tumor burden a greater amount of CXCR4⁺ exosomes could be detected in circulation. However, since KPC 844 was the

one with a greater tumor burden this hypothesis does not seem to be true. To further confirm our findings, CXCR4 expression analysis on KPC mice pancreas and liver (site of metastasis) was performed. According to our results, only a very small subset of pancreatic cancer cells expresses CXCR4 in the primary tumors of the KPC mice. This further confirms the CXCR4 association with a stem cell marker, since cancer stem cells are usually present in low abundance in a tumor. Taking this in consideration, due to the low number of pancreatic cancer cells that express CXCR4 is expected that no differences are observed in the number of CXCR4⁺ exosomes in circulation between the different stages of disease progression.

5.CONCLUSION AND FUTURE PERSPECTIVES

The role of exosomes in cancer has been well studied in the past years and several papers in the literature suggest their involvement in various tumorigenic processes. However, there are still important features of these structures that are not yet known and despite the advances, the techniques currently used to study exosomes are still very limited. In this study, we proposed a mechanism of communication between cancer cells and future metastatic organs. Exosomes produced by cancer cells travel through the circulation system and are taken up by recipient cells. The mechanism that determines which cells receive these exosomes is unknown. Cells can select the cargo that is loaded into exosomes. The fact that this loading is not random may indicate that the cells produce exosomes for different effects. We hypothesise that the presence of CXCR4 in cancer exosomes facilitated their retention at CXCL12-enriched organs promoting effective metastatic colonization at those organs. It has already been proven that this mechanism occurs in tumor cells of various types of cancer. The idea would be to prove that cancer cells send exosomes to certain organs, prepare the tissue to receive cancer cells and then colonize the organ to form metastasis. It has already been proved that the common site of metastasis of several cancer types, including pancreatic cancer, are CXCL12-producing organs. Our study shows that tumors that overexpress CXCR4 are more aggressive and that these cells produce exosomes that also express CXCR4. The experience should be repeated since the loss of animals during the experience made it difficult to obtain results with statistical power. This experiment is not conclusive, however our results suggest that this protein might have an important biological significance in these structures and their role should be assessed.

REFERENCES

- Al-Nedawi, K., Meehan, B., Kerbel, R. S., Allison, A. C., & Rak, J. (2009). Endothelial expression of autocrine VEGF upon the uptake of tumor-derived microvesicles containing oncogenic EGFR. *Proceedings of the National Academy of Sciences*, *106*(10), 3794–3799. <http://doi.org/10.1073/pnas.0804543106>
- Andreu, Z., & Yáñez-Mó, M. (2014). Tetraspanins in extracellular vesicle formation and function. *Frontiers in Immunology*, *5*, 442. <http://doi.org/10.3389/fimmu.2014.00442>
- Arora, S., Bhardwaj, A., Singh, S., Srivastava, S. K., McClellan, S., Nirodi, C. S., ... Singh, A. P. (2013). An undesired effect of chemotherapy: gemcitabine promotes pancreatic cancer cell invasiveness through reactive oxygen species-dependent, nuclear factor κ B- and hypoxia-inducible factor 1 α -mediated up-regulation of CXCR4. *The Journal of Biological Chemistry*, *288*(29), 21197–207. <http://doi.org/10.1074/jbc.M113.484576>
- Atay, S., & Godwin, A. K. (2014). Tumor-derived exosomes: A message delivery system for tumor progression. *Communicative & Integrative Biology*, *7*(1), e28231. <http://doi.org/10.4161/cib.28231>
- Baglio, S. R., Lagerweij, T., Pérez Lanzón, M., Xuan Ho, D., Léveillé, N., Melo, S. A., ... Pegtel, D. M. (2017). Blocking tumor-educated MSC paracrine activity halts osteosarcoma progression. *Clinical Cancer Research*. Retrieved from <http://clincancerres.aacrjournals.org/content/early/2017/01/04/1078-0432.CCR-16-2726.full-text.pdf>
- Balic, A., Dorado, J., Alonso-Gómez, M., & Heeschen, C. (2012). Stem cells as the root of pancreatic ductal adenocarcinoma. *Experimental Cell Research*, *318*, 691–704. <http://doi.org/10.1016/j.yexcr.2011.11.007>
- Balkwill, F. (2004a). Cancer and the chemokine network. *Nature Reviews Cancer*, *4*(7), 540–550. <http://doi.org/10.1038/nrc1388>
- Balkwill, F. (2004b). The significance of cancer cell expression of the chemokine receptor CXCR4. *Seminars in Cancer Biology*, *14*, 171–179. <http://doi.org/10.1016/j.semcan.2003.10.003>

- Batagov, A. O., Kuznetsov, V. A., & Kurochkin, I. V. (2011). Identification of nucleotide patterns enriched in secreted RNAs as putative cis-acting elements targeting them to exosome nanovesicles. *BMC Genomics*, *12 Suppl 3*(Suppl 3), S18. <http://doi.org/10.1186/1471-2164-12-S3-S18>
- Biankin, A. V., Waddell, N., Kassahn, K. S., Gingras, M.-C., Muthuswamy, L. B., Johns, A. L., ... Grimmond, S. M. (2012). Pancreatic cancer genomes reveal aberrations in axon guidance pathway genes. *Nature*, *491*(7424), 399–405. <http://doi.org/10.1038/nature11547>
- Bilimoria, K. Y., Bentrem, D. J., Ko, C. Y., Ritchey, J., Stewart, A. K., Winchester, D. P., & Talamonti, M. S. (2007). Validation of the 6th edition AJCC pancreatic cancer staging system. *Cancer*, *110*(4), 738–744. <http://doi.org/10.1002/cncr.22852>
- Burger, J. A., & Kipps, T. J. (2006). CXCR4 : a key receptor in the crosstalk between tumor cells and their microenvironment. *Blood*, *107*(5), 1761–1767. <http://doi.org/10.1182/blood-2005-08-3182>
- Buschow, S. I., Liefhebber, J. M. P., Wubbolts, R., & Stoorvogel, W. (2005). Exosomes contain ubiquitinated proteins. *Blood Cells, Molecules, and Diseases*, *35*(3), 398–403. <http://doi.org/10.1016/j.bcmd.2005.08.005>
- Busillo, J. M., & Benovic, J. L. (2007). Regulation of CXCR4 signaling. *Biochimica et Biophysica Acta*, *1768*(4), 952–63. <http://doi.org/10.1016/j.bbamem.2006.11.002>
- Camussi, G., Deregibus, M. C., Bruno, S., Cantaluppi, V., & Biancone, L. (2010). Exosomes / microvesicles as a mechanism of cell-to-cell communication. *Kidney International*, *78*(9), 838–848. <http://doi.org/10.1038/ki.2010.278>
- Cancer. (2017). Retrieved July 2, 2017, from <http://www.who.int/mediacentre/factsheets/fs297/en/>
- Castellanos, J. A., Merchant, N. B., & Nagathihalli, N. S. (2013). Emerging targets in pancreatic cancer: epithelial-mesenchymal transition and cancer stem cells. *OncoTargets and Therapy*, *6*, 1261–7. <http://doi.org/10.2147/OTT.S34670>
- Cepeda, E. B., Dediulia, T., Fernando, J., Bertran, E., Egea, G., Navarro, E., & Fabregat, I. (2015). Mechanisms regulating cell membrane localization of the chemokine receptor CXCR4 in human hepatocarcinoma cells. *Biochimica et Biophysica Acta (BBA) - Molecular Cell*

- Research*, 1853(5), 1205–1218. <http://doi.org/10.1016/j.bbamcr.2015.02.012>
- Chang, D. K., Grimmond, S. M., & Biankin, A. V. (2014). Pancreatic cancer genomics. *Current Opinion in Genetics & Development*, 24, 74–81. <http://doi.org/10.1016/J.GDE.2013.12.001>
- Chang, Q., Bournazou, E., Sansone, P., Berishaj, M., Gao, S. P., Daly, L., ... Bromberg, J. (2013). The IL-6/JAK/Stat3 feed-forward loop drives tumorigenesis and metastasis. *Neoplasia (New York, N.Y.)*, 15(7), 848–62. Retrieved from <http://www.ncbi.nlm.nih.gov/pubmed/23814496>
- Charo, I. F., & Ransohoff, R. M. (2006). The Many Roles of Chemokines and Chemokine Receptors in Inflammation. *New England Journal of Medicine*, 354(6), 610–621. <http://doi.org/10.1056/NEJMra052723>
- Chen, G., Wang, W., Meng, S., Zhang, L., Wang, W., Jiang, Z., ... Li, M. (2014). CXC chemokine CXCL12 and its receptor CXCR4 in tree shrews (*Tupaia belangeri*): structure, expression and function. *PloS One*, 9(5), e98231. <http://doi.org/10.1371/journal.pone.0098231>
- Chevallier, J., Chamoun, Z., Jiang, G., Prestwich, G., Sakai, N., Matile, S., ... Gruenberg, J. (2008). Lyso-bisphosphatidic acid controls endosomal cholesterol levels. *The Journal of Biological Chemistry*, 283(41), 27871–80. <http://doi.org/10.1074/jbc.M801463200>
- Colombo, M., Moita, C., van Niel, G., Kowal, J., Vigneron, J., Benaroch, P., ... Raposo, G. (2013). Analysis of ESCRT functions in exosome biogenesis, composition and secretion highlights the heterogeneity of extracellular vesicles. *Journal of Cell Science*, 126(24), 5553–5565. <http://doi.org/10.1242/jcs.128868>
- Colombo, M., Raposo, G., & Théry, C. (2014). Biogenesis, Secretion, and Intercellular Interactions of Exosomes and Other Extracellular Vesicles. *Annu. Rev. Cell Dev. Biol*, 30, 255–89. <http://doi.org/10.1146/annurev-cellbio-101512-122326>
- Costa-silva, B., Aiello, N. M., Ocean, A. J., Singh, S., Zhang, H., Thakur, B. K., ... Ebbesen, S. H. (2015). Pancreatic cancer exosomes initiate pre-metastatic niche formation in the liver. *Nature Cell Biology*, 17(6), 816–826. <http://doi.org/10.1038/ncb3169>
- Croswell, J. M., Ransohoff, D. F., & Kramer, B. S. (2010). Principles of cancer screening: lessons from history and study design issues. *Seminars in Oncology*, 37(3), 202–15.

<http://doi.org/10.1053/j.seminoncol.2010.05.006>

- Crump, M. P., Gong, J. H., Loetscher, P., Rajarathnam, K., Amara, A., Arenzana-Seisdedos, F., ... Clark-Lewis, I. (1997). Solution structure and basis for functional activity of stromal cell-derived factor-1; dissociation of CXCR4 activation from binding and inhibition of HIV-1. *The EMBO Journal*, *16*(23), 6996–7007. <http://doi.org/10.1093/emboj/16.23.6996>
- Dabitao, D., Margolick, J. B., Lopez, J., & Bream, J. H. (2011). Multiplex measurement of proinflammatory cytokines in human serum: Comparison of the Meso Scale Discovery electrochemiluminescence assay and the Cytometric Bead Array. *Journal of Immunological Methods*, *372*(1-2), 71–77. <http://doi.org/10.1016/j.jim.2011.06.033>
- Essandoh, K., Yang, L., Wang, X., Huang, W., Qin, D., Hao, J., ... Fan, G.-C. (2015). Blockade of exosome generation with GW4869 dampens the sepsis-induced inflammation and cardiac dysfunction. *Biochimica et Biophysica Acta*, *1852*(11), 2362–71. <http://doi.org/10.1016/j.bbadis.2015.08.010>
- Feig, C., Gopinathan, A., Neesse, A., Chan, D. S., Cook, N., & Tuveson, D. A. (2012). The pancreas cancer microenvironment. *Clinical Cancer Research: An Official Journal of the American Association for Cancer Research*, *18*(16), 4266–76. <http://doi.org/10.1158/1078-0432.CCR-11-3114>
- Gould, G. W., & Lippincott-Schwartz, J. (2009). New roles for endosomes: from vesicular carriers to multi-purpose platforms. *Nature Reviews Molecular Cell Biology*, *10*(4), 287–292. <http://doi.org/10.1038/nrm2652>
- Gupta, S. K., Lysko, P. G., Pillarisetti, K., Ohlstein, E., & Stadel, J. M. (1998). Chemokine receptors in human endothelial cells. Functional expression of CXCR4 and its transcriptional regulation by inflammatory cytokines. *The Journal of Biological Chemistry*, *273*(7), 4282–7. Retrieved from <http://www.ncbi.nlm.nih.gov/pubmed/9461627>
- Hanahan, D., & Weinberg, R. A. (2000). The hallmarks of cancer. *Cell*, *100*(1), 57–70. <http://doi.org/10.1007/s00262-010-0968-0>
- Hanahan, D., & Weinberg, R. A. (2011). Hallmarks of cancer: The next generation. *Cell*, *144*(5), 646–674. <http://doi.org/10.1016/j.cell.2011.02.013>
- Haribabu, B., Richardson, R. M., Fisher, I., Sozzani, S., Peiper, S. C., Horuk, R., ... Snyderman, R.

- (1997). Regulation of human chemokine receptors CXCR4. Role of phosphorylation in desensitization and internalization. *The Journal of Biological Chemistry*, 272(45), 28726–31. Retrieved from <http://www.ncbi.nlm.nih.gov/pubmed/9353342>
- Hart2, I. R., & Fidler, I. J. (1980). *Role of Organ Selectivity in the Determination of Metastatic Patterns of B16 Melanoma*. *CANCER RESEARCH* (Vol. 40). Retrieved from <http://cancerres.aacrjournals.org/content/40/7/2281.full-text.pdf>
- Hermann, P. C., Huber, S. L., Herrler, T., Aicher, A., Ellwart, J. W., Guba, M., ... Heeschen, C. (2007). Distinct Populations of Cancer Stem Cells Determine Tumor Growth and Metastatic Activity in Human Pancreatic Cancer. *Cell Stem Cell*, 1(3), 313–323. <http://doi.org/10.1016/J.STEM.2007.06.002>
- Hezel, A. F., Kimmelman, A. C., Stanger, B. Z., Bardeesy, N., & Depinho, R. A. (2006). Genetics and biology of pancreatic ductal adenocarcinoma. *Genes & Development*, 20(10), 1218–1249. <http://doi.org/10.1101/gad.1415606>
- Hingorani, S. R., Petricoin, E. F., Maitra, A., Rajapakse, V., King, C., Jacobetz, M. A., ... Tuveson, D. A. (2003). Preinvasive and invasive ductal pancreatic cancer and its early detection in the mouse. *Cancer Cell*, 4(6), 437–50. Retrieved from <http://www.ncbi.nlm.nih.gov/pubmed/14706336>
- Hingorani, S. R., Wang, L., Multani, A. S., Combs, C., Deramaudt, T. B., Hruban, R. H., ... Tuveson, D. A. (2005). Trp53R172H and KrasG12D cooperate to promote chromosomal instability and widely metastatic pancreatic ductal adenocarcinoma in mice. *Cancer Cell*, 7(5), 469–483. <http://doi.org/10.1016/j.ccr.2005.04.023>
- Hood, J. L., San, R. S., & Wickline, S. A. (2011). Exosomes Released by Melanoma Cells Prepare Sentinel Lymph Nodes for Tumor Metastasis. *Cancer Research*, 71(11), 3792–3801. <http://doi.org/10.1158/0008-5472.CAN-10-4455>
- Hoshino, A., Costa-silva, B., Shen, T., Rodrigues, G., Hashimoto, A., Mark, M. T., ... Ever. (2015). Tumour exosome integrins determine organotropic metastasis. *Nature*, 527(7578), 329–335. <http://doi.org/10.1038/nature15756>
- Hruban, R. H., Adsay, N. V., Albores-Saavedra, J., Anver, M. R., Biankin, A. V., Boivin, G. P., ... Tuveson, D. A. (2006). Pathology of Genetically Engineered Mouse Models of Pancreatic

- Exocrine Cancer: Consensus Report and Recommendations. *Cancer Research*, 66(1), 95–106. <http://doi.org/10.1158/0008-5472.CAN-05-2168>
- Hurley, J. H., & Hanson, P. I. (2010). Membrane budding and scission by the ESCRT machinery: it's all in the neck. *Nature Reviews Molecular Cell Biology*, 11(8), 556–566. <http://doi.org/10.1038/nrm2937>
- Ikonen, E. (2001). Roles of lipid rafts in membrane transport. *Current Opinion in Cell Biology*, 13(4), 470–7. Retrieved from <http://www.ncbi.nlm.nih.gov/pubmed/11454454>
- Johnstone, R. M., Adam, M., Hammond, J. R., Orr, L., & Turbide, C. (1987). Vesicle formation during reticulocyte maturation. Association of plasma membrane activities with released vesicles (exosomes). *The Journal of Biological Chemistry*, 262(19), 9412–20. Retrieved from <http://www.ncbi.nlm.nih.gov/pubmed/3597417>
- Jourdan, P., Vendrell, J. P., Huguet, M. F., Segondy, M., Bousquet, J., Pène, J., & Yssel, H. (2000). Cytokines and cell surface molecules independently induce CXCR4 expression on CD4+ CCR7+ human memory T cells. *Journal of Immunology (Baltimore, Md. : 1950)*, 165(2), 716–24. Retrieved from <http://www.ncbi.nlm.nih.gov/pubmed/10878344>
- Kahlert, C., Melo, S. A., Protopopov, A., Tang, J., Seth, S., Koch, M., ... Kalluri, R. (2014). Identification of double-stranded genomic DNA spanning all chromosomes with mutated KRAS and p53 DNA in the serum exosomes of patients with pancreatic cancer. *The Journal of Biological Chemistry*, 289(7), 3869–75. <http://doi.org/10.1074/jbc.C113.532267>
- Kaplan, R. N., Rafii, S., & Lyden, D. (2006). Preparing the “soil”: The Premetastatic niche. *Cancer Research*, 66(23), 11089–11093. <http://doi.org/10.1158/0008-5472.CAN-06-2407>
- Kaplan, R. N., Riba, R. D., Zacharoulis, S., Anna, H., Vincent, L., Costa, C., ... Lyden, D. (2005). VEGFR1-positive haematopoietic bone marrow progenitors initiate the pre-metastatic niche. *Nature*, 438(7069), 820–827. <http://doi.org/10.1038/nature04186>
- Keustermans, G. C. E., Hoeks, S. B. E., Meerding, J. M., Prakken, B. J., & de Jager, W. (2013). Cytokine assays: An assessment of the preparation and treatment of blood and tissue samples. *Methods*, 61(1), 10–17. <http://doi.org/10.1016/j.ymeth.2013.04.005>
- Kleeff, J., Korc, M., Apte, M., La Vecchia, C., Johnson, C. D., Biankin, A. V., ... Neoptolemos, J. P. (2016). Pancreatic cancer. *Nature Reviews Disease Primers*, 2, 16022.

<http://doi.org/10.1038/nrdp.2016.22>

- Klumperman, J., & Raposo, G. (2014). The Complex Ultrastructure of the Endolysosomal System. *Cold Spring Harbor Perspectives in Biology*, 6(10), a016857–a016857. <http://doi.org/10.1101/cshperspect.a016857>
- Kowal, J., Arras, G., Colombo, M., Jouve, M., Morath, J. P., Primdal-Bengtson, B., ... Théry, C. (2016). Proteomic comparison defines novel markers to characterize heterogeneous populations of extracellular vesicle subtypes. *Proceedings of the National Academy of Sciences*, 113(8), E968–E977. <http://doi.org/10.1073/pnas.1521230113>
- Labori, K. J., Katz, M. H., Tzeng, C. W., Bjørneth, B. A., Cvancarova, M., Edwin, B., ... Gladhaug, I. P. (2016). Impact of early disease progression and surgical complications on adjuvant chemotherapy completion rates and survival in patients undergoing the surgery first approach for resectable pancreatic ductal adenocarcinoma – A population-based cohort study. *Acta Oncologica*, 55(3), 265–277. <http://doi.org/10.3109/0284186X.2015.1068445>
- Lapham, C. K., Romantseva, T., Petricoin, E., King, L. R., Manischewitz, J., Zaitseva, M. B., & Golding, H. (2002). CXCR4 heterogeneity in primary cells: possible role of ubiquitination. *Journal of Leukocyte Biology*, 72(6), 1206–14. Retrieved from <http://www.ncbi.nlm.nih.gov/pubmed/12488503>
- Lee, T. H., Asti, E. D., & Magnus, N. (2011). Microvesicles as mediators of intercellular communication in cancer – the emerging science of cellular “ debris ,” 455–467. <http://doi.org/10.1007/s00281-011-0250-3>
- Li, Y. M., Pan, Y., Wei, Y., Cheng, X., Zhou, B. P., Tan, M., ... Hung, M.-C. (2004). Upregulation of CXCR4 is essential for HER2-mediated tumor metastasis. *Cancer Cell*, 6(5), 459–469. <http://doi.org/10.1016/j.ccr.2004.09.027>
- Li, Z. (2013). CD133: a stem cell biomarker and beyond. *Experimental Hematology & Oncology*, 2(1), 17. <http://doi.org/10.1186/2162-3619-2-17>
- Llorente, A., Skotland, T., Sylvänne, T., Kauhanen, D., Róg, T., Orłowski, A., ... Sandvig, K. (2013). Molecular lipidomics of exosomes released by PC-3 prostate cancer cells. *Biochimica et Biophysica Acta*, 1831(7), 1302–9. Retrieved from <http://www.ncbi.nlm.nih.gov/pubmed/24046871>

- Lu, X., & Kang, Y. (2007). Organotropism of Breast Cancer Metastasis. *Journal of Mammary Gland Biology and Neoplasia*, *12*(2-3), 153–162. <http://doi.org/10.1007/s10911-007-9047-3>
- Luzzi, K. J., MacDonald, I. C., Schmidt, E. E., Kerkvliet, N., Morris, V. L., Chambers, A. F., & Groom, A. C. (1998). Multistep nature of metastatic inefficiency: dormancy of solitary cells after successful extravasation and limited survival of early micrometastasis. *The American Journal of Pathology*, *153*(3), 865–73. [http://doi.org/10.1016/S0002-9440\(10\)65628-3](http://doi.org/10.1016/S0002-9440(10)65628-3)
- Marchese, A., & Benovic, J. L. (2001). Agonist-promoted Ubiquitination of the G Protein-coupled Receptor CXCR4 Mediates Lysosomal Sorting. *Journal of Biological Chemistry*, *276*(49), 45509–45512. <http://doi.org/10.1074/jbc.C100527200>
- Marchese, A., Chen, C., Kim, Y.-M., & Benovic, J. L. (2003). The ins and outs of G protein-coupled receptor trafficking. *Trends in Biochemical Sciences*, *28*(7), 369–376. [http://doi.org/10.1016/S0968-0004\(03\)00134-8](http://doi.org/10.1016/S0968-0004(03)00134-8)
- Marchesi, F., Monti, P., Leone, B. E., Zerbi, A., Vecchi, A., Piemonti, L., ... Allavena, P. (2004). Increased Survival, Proliferation, and Migration in Metastatic Human Pancreatic Tumor Cells Expressing Functional CXCR4. *Cancer Research*, *64*(22), 8420–8427. <http://doi.org/10.1158/0008-5472.CAN-04-1343>
- Maréchal, R., Demetter, P., Nagy, N., Berton, A., Decaestecker, C., Polus, M., ... Van Laethem, J.-L. (2009). High expression of CXCR4 may predict poor survival in resected pancreatic adenocarcinoma. *British Journal of Cancer*, *100*(9), 1444–51. <http://doi.org/10.1038/sj.bjc.6605020>
- Martins, V. R., Dias, M. S., & Hainaut, P. (2013). Tumor-cell-derived microvesicles as carriers of molecular information in cancer. *Current Opinion in Oncology*, *25*(1), 66–75. <http://doi.org/10.1097/CCO.0b013e32835b7c81>
- Meldolesi, J. (2018). Exosomes and Ectosomes in Intercellular Communication. *Current Biology*, *28*(8), R435–R444. <http://doi.org/10.1016/j.cub.2018.01.059>
- Melo, S. A., Luecke, L. B., Kahlert, C., Fernandez, A. F., Gammon, S. T., Kaye, J., ... Kalluri, R. (2015). Glypican-1 identifies cancer exosomes and detects early pancreatic cancer. *Nature*, *523*(7559), 177–182. <http://doi.org/10.1038/nature14581>
- Melo, S. A., Sugimoto, H., Connell, J. T. O., Kato, N., Villanueva, A., Vidal, A., ... Calin, G. A. (2014).

- Exosomes perform cell-independent microRNA biogenesis and promote tumorigenesis. *Cancer Cell*, 26(5), 707–721. <http://doi.org/10.1016/j.ccell.2014.09.005>
- Mori, T., Doi, R., Koizumi, M., Toyoda, E., Ito, D., Kami, K., ... Imamura, M. (2004). CXCR4 antagonist inhibits stromal cell-derived factor 1-induced migration and invasion of human pancreatic cancer. *Molecular Cancer Therapeutics*, 3(1), 29–37.
- Moriuchi, M., Moriuchi, H., Turner, W., & Fauci, A. S. (1997). Cloning and analysis of the promoter region of CXCR4, a coreceptor for HIV-1 entry. *Journal of Immunology (Baltimore, Md. : 1950)*, 159(9), 4322–9. Retrieved from <http://www.ncbi.nlm.nih.gov/pubmed/9379028>
- Murphy, P. M. (1994). The Molecular Biology of Leukocyte Chemoattractant Receptors. *Annual Review of Immunology*, 12(1), 593–633. <http://doi.org/10.1146/annurev.iy.12.040194.003113>
- Murphy, P. M., Baggiolini, M., Charo, I. F., Hébert, C. A., Horuk, R., Matsushima, K., ... Power, C. A. (2000). International union of pharmacology. XXII. Nomenclature for chemokine receptors. *Pharmacological Reviews*, 52(1), 145–76. Retrieved from <http://www.ncbi.nlm.nih.gov/pubmed/10699158>
- Neesse, A., Michl, P., Frese, K. K., Feig, C., Cook, N., Jacobetz, M. A., ... Tuveson, D. A. (2011). Stromal biology and therapy in pancreatic cancer. *Gut*, 60(6), 861–8. <http://doi.org/10.1136/gut.2010.226092>
- Orsini, M. J., Parent, J.-L., Mundell, S. J., & Benovic, J. L. (1999). Trafficking of the HIV Coreceptor CXCR4. *Journal of Biological Chemistry*, 274(43), 31076–31086. <http://doi.org/10.1074/JBC.274.43.31076>
- Ostrowski, M., Carmo, N. B., Krumeich, S., Fanget, I., Raposo, G., Savina, A., ... Thery, C. (2010). Rab27a and Rab27b control different steps of the exosome secretion pathway. *Nature Cell Biology*, 12(1), 19–30; sup pp 1–13. <http://doi.org/10.1038/ncb2000>
- Paget, S. (1889). The distribution of secondary growths in cancer of the breast. *The Lancet*, 133(3421), 571–573. [http://doi.org/10.1016/S0140-6736\(00\)49915-0](http://doi.org/10.1016/S0140-6736(00)49915-0)
- Peinado, H., Alec, M., Lavotshkin, S., Matei, I., Costa-silva, B., Moreno-bueno, G., ... Kang, Y. (2012). Melanoma exosomes educate bone marrow progenitor cells toward a pro-metastatic phenotype through MET. *Nature Medicine*, 18(6), 883–891.

<http://doi.org/10.1038/nm.2753>

- Peinado, H., Lavotshkin, S., & Lyden, D. (2011). The secreted factors responsible for pre-metastatic niche formation : Old sayings and new thoughts. *Seminars in Cancer Biology*, *21*(2), 139–146. <http://doi.org/10.1016/j.semcancer.2011.01.002>
- Peinado, H., Zhang, H., Matei, I. R., Costa-Silva, B., Hoshino, A., Rodrigues, G., ... Lyden, D. (2017). Pre-metastatic niches: organ-specific homes for metastasis. *Nature Reviews Cancer*, *17*(5), 302–317. <http://doi.org/10.1038/nrc.2017.6>
- Pietras, K., & Östman, A. (2010). Hallmarks of cancer: Interactions with the tumor stroma. *Experimental Cell Research*, *316*(8), 1324–1331. <http://doi.org/10.1016/j.yexcr.2010.02.045>
- Premack, B. A., & Schall, T. J. (1996). Chemokine receptors: Gateways to inflammation and infection. *Nature Medicine*, *2*(11), 1174–1178. <http://doi.org/10.1038/nm1196-1174>
- Psaila, B., & Lyden, D. (2009). The metastatic niche: adapting the foreign soil. *Nature Reviews Cancer*, *9*(4), 285–293. <http://doi.org/10.1038/nrc2621>
- Rak, J., & Guha, A. (2012). Extracellular vesicles - vehicles that spread cancer genes. *BioEssays*, *34*(6), 489–497. <http://doi.org/10.1002/bies.201100169>
- Ratajczak, J., Wysoczynski, M., Hayek, F., Janowska-Wieczorek, A., & Ratajczak, M. Z. (2006). Membrane-derived microvesicles: important and underappreciated mediators of cell-to-cell communication. *Leukemia*, *20*(9), 1487–1495. <http://doi.org/10.1038/sj.leu.2404296>
- Ruivo, C. F., Adem, B., Silva, M., & Melo, S. A. (2017). The Biology of Cancer Exosomes: Insights and New Perspectives. *Cancer Research*, *77*(23), 6480–6488. <http://doi.org/10.1158/0008-5472.CAN-17-0994>
- Sato-Kuwabara, Y., Melo, S. A., Soares, F. A., & Calin, G. A. (2015). The fusion of two worlds: non-coding RNAs and extracellular vesicles—diagnostic and therapeutic implications (Review). *International Journal of Oncology*, *46*(1), 17–27. <http://doi.org/10.3892/ijo.2014.2712>
- Sceneay, J., Smyth, M. J., & Möller, A. (2013). The pre-metastatic niche: Finding common ground. *Cancer and Metastasis Reviews*, *32*(3-4), 449–464. <http://doi.org/10.1007/s10555-013-9420-1>

- Schuler, P. J., Saze, Z., Hong, C.-S., Muller, L., Gillespie, D. G., Cheng, D., ... Whiteside, T. L. (2014). Human CD4⁺ CD39⁺ regulatory T cells produce adenosine upon co-expression of surface CD73 or contact with CD73⁺ exosomes or CD73⁺ cells. *Clinical and Experimental Immunology*, *177*(2), 531–43. <http://doi.org/10.1111/cei.12354>
- Siegel, R., Ma, J., Zou, Z., & Jemal, A. (2014). Cancer statistics, 2014. *CA: A Cancer Journal for Clinicians*, *64*(1), 9–29. <http://doi.org/10.3322/caac.21208>
- Signoret, N., Oldridge, J., Pelchen-Matthews, A., Klasse, P. J., Tran, T., Brass, L. F., ... Marsh, M. (1997). Phorbol esters and SDF-1 induce rapid endocytosis and down modulation of the chemokine receptor CXCR4. *The Journal of Cell Biology*, *139*(3), 651–64. <http://doi.org/10.1083/JCB.139.3.651>
- Singh, S., Sadanandam, A., & Singh, R. K. (2007). Chemokines in tumor angiogenesis and metastasis. *Cancer and Metastasis Reviews*, *26*(3-4), 453–467. <http://doi.org/10.1007/s10555-007-9068-9>
- Singh, S., Srivastava, S. K., Bhardwaj, A., Owen, L. B., & Singh, A. P. (2010). CXCL12-CXCR4 signalling axis confers gemcitabine resistance to pancreatic cancer cells: a novel target for therapy. *British Journal of Cancer*, *103*(11), 1671–9. <http://doi.org/10.1038/sj.bjc.6605968>
- Skog, J., Würdinger, T., van Rijn, S., Meijer, D. H., Gainche, L., Sena-Esteves, M., ... Breakefield, X. O. (2008). Glioblastoma microvesicles transport RNA and proteins that promote tumour growth and provide diagnostic biomarkers. *Nature Cell Biology*, *10*(12), 1470–6. <http://doi.org/10.1038/ncb1800>
- Sleeman, J. P. (2012). The metastatic niche and stromal progression. *Cancer Metastasis Reviews*, *31*(3-4), 429–40. <http://doi.org/10.1007/s10555-012-9373-9>
- Sleightholm, R. L., Neilsen, B. K., Li, J., Steele, M. M., Singh, R. K., Hollingsworth, M. A., & Oupicky, D. (2017). Emerging roles of the CXCL12/CXCR4 axis in pancreatic cancer progression and therapy. *Pharmacology & Therapeutics*, *179*, 158–170. <http://doi.org/10.1016/j.pharmthera.2017.05.012>
- Sohn, T. A., & Yeo, C. J. (2000). The molecular genetics of pancreatic ductal carcinoma: a review. *Surgical Oncology*, *9*(3), 95–101. Retrieved from

<http://www.ncbi.nlm.nih.gov/pubmed/11356337>

- Soung, Y. H., Nguyen, T., Cao, H., Lee, J., & Chung, J. (2015). Emerging roles of exosomes in cancer invasion and metastasis. *BMB Reports*, *49*(1), 18–25. <http://doi.org/10.5483/BMBRep.2016.49.1.239>
- Stoorvogel, W., Strous, G. J., Geuze, H. J., Oorschot, V., & Schwartz, A. L. (1991). Late endosomes derive from early endosomes by maturation. *Cell*, *65*(3), 417–27. Retrieved from <http://www.ncbi.nlm.nih.gov/pubmed/1850321>
- Sun, X., Cheng, G., Hao, M., Zheng, J., Zhou, X., Zhang, J., ... Wang, J. (2010). CXCL12/CXCR4/CXCR7 Chemokine Axis and Cancer Progression. *Cancer and Metastasis Reviews*, *29*(4), 709–722. <http://doi.org/10.1007/s10555-010-9256-x>
- Szczepanski, M. J., Szajnik, M., Welsh, A., Whiteside, T. L., & Boyiadzis, M. (2011). Blast-derived microvesicles in sera from patients with acute myeloid leukemia suppress natural killer cell function via membrane-associated transforming growth factor-1. *Haematologica*, *96*(9), 1302–1309. <http://doi.org/10.3324/haematol.2010.039743>
- Tanaka, M. (2014). Thirty Years of Experience with Intraductal Papillary Mucinous Neoplasm of the Pancreas: From Discovery to International Consensus. *Digestion*, *90*(4), 265–272. <http://doi.org/10.1159/000370111>
- Thakur, B. K., Zhang, H., Becker, A., Matei, I., Huang, Y., Costa-Silva, B., ... Lyden, D. (2014). Double-stranded DNA in exosomes: a novel biomarker in cancer detection. *Cell Research*, *24*(6), 766–9. <http://doi.org/10.1038/cr.2014.44>
- Théry, C., Zitvogel, L., & Amigorena, S. (2002). Exosomes: composition, biogenesis and function. *Nature Reviews Immunology*, *2*(8), 569–579. <http://doi.org/10.1038/nri855>
- Tricarico, C., Clancy, J., & D'Souza-Schorey, C. (2017). Biology and biogenesis of shed microvesicles. *Small GTPases*, *8*(4), 220–232. <http://doi.org/10.1080/21541248.2016.1215283>
- Valadi, H., Ekström, K., Bossios, A., Sjöstrand, M., Lee, J. J., & Lötval, J. O. (2007). Exosome-mediated transfer of mRNAs and microRNAs is a novel mechanism of genetic exchange between cells. *Nature Cell Biology*, *9*(6), 654–659. <http://doi.org/10.1038/ncb1596>
- van der Pol, E., Boing, A. N., Harrison, P., Sturk, A., & Nieuwland, R. (2012). Classification,

- Functions, and Clinical Relevance of Extracellular Vesicles. *Pharmacological Reviews*, *64*(3), 676–705. <http://doi.org/10.1124/pr.112.005983>
- van Niel, G., D'Angelo, G., & Raposo, G. (2018). Shedding light on the cell biology of extracellular vesicles. *Nature Reviews Molecular Cell Biology*, *19*(4), 213–228. <http://doi.org/10.1038/nrm.2017.125>
- Vandercappellen, J., Van Damme, J., & Struyf, S. (2008). The role of CXC chemokines and their receptors in cancer. *Cancer Letters*, *267*(2), 226–244. <http://doi.org/10.1016/j.canlet.2008.04.050>
- Wasmuth, E. V., Januszyk, K., & Lima, C. D. (2014). Structure of an Rrp6–RNA exosome complex bound to poly(A) RNA. *Nature*, *511*(7510), 435–439. <http://doi.org/10.1038/nature13406>
- Westphalen, C. B., & Olive, K. P. (2012a). Genetically Engineered Mouse Models of Pancreatic Cancer. *The Cancer Journal*, *18*(6), 502–510. <http://doi.org/10.1097/PPO.0b013e31827ab4c4>
- Westphalen, C. B., & Olive, K. P. (2012b). Genetically engineered mouse models of pancreatic cancer. *Cancer Journal (Sudbury, Mass.)*, *18*(6), 502–10. <http://doi.org/10.1097/PPO.0b013e31827ab4c4>
- White, M. C., Holman, D. M., Boehm, J. E., Peipins, L. A., Grossman, M., & Henley, S. J. (2014). Age and cancer risk: a potentially modifiable relationship. *American Journal of Preventive Medicine*, *46*(3 Suppl 1), S7–15. <http://doi.org/10.1016/j.amepre.2013.10.029>
- Whiteside, T. L. (2010). Immune responses to malignancies. *The Journal of Allergy and Clinical Immunology*, *125*(2 Suppl 2), S272–83. <http://doi.org/10.1016/j.jaci.2009.09.045>
- Whiteside, T. L. (2016). Tumor-Derived Exosomes and Their Role in Cancer Progression. *Advances in Clinical Chemistry*, *74*, 103–41. <http://doi.org/10.1016/bs.acc.2015.12.005>
- Wieckowski, E. U., Visus, C., Szajnik, M., Szczepanski, M. J., Storkus, W. J., & Whiteside, T. L. (2009). Tumor-derived microvesicles promote regulatory T cell expansion and induce apoptosis in tumor-reactive activated CD8+ T lymphocytes. *Journal of Immunology (Baltimore, Md. : 1950)*, *183*(6), 3720–30. <http://doi.org/10.4049/jimmunol.0900970>
- Wubbolts, R., Leckie, R. S., Veenhuizen, P. T. M., Schwarzmann, G., Möbius, W., Hoernschemeyer, J., ... Stoorvogel, W. (2003). Proteomic and biochemical analyses of human B cell-derived

- exosomes. Potential implications for their function and multivesicular body formation. *The Journal of Biological Chemistry*, *278*(13), 10963–72. <http://doi.org/10.1074/jbc.M207550200>
- Xia, J., Chen, C., Chen, Z., Miele, L., Sarkar, F. H., & Wang, Z. (2012). Targeting pancreatic cancer stem cells for cancer therapy. *Biochimica et Biophysica Acta (BBA) - Reviews on Cancer*, *1826*(2), 385–399. <http://doi.org/10.1016/J.BBCAN.2012.06.002>
- Zappulli, V., Friis, K. P., Fitzpatrick, Z., Maguire, C. A., & Breakefield, X. O. (2016). Extracellular vesicles and intercellular communication within the nervous system, *126*(4). <http://doi.org/10.1172/JCI81134>.The
- Zhang, Y., Foudi, A., Geay, J.-F., Berthebaud, M., Buet, D., Jarrier, P., ... Louache, F. (2004). Intracellular Localization and Constitutive Endocytosis of CXCR4 in Human CD34 + Hematopoietic Progenitor Cells. *Stem Cells*, *22*(6), 1015–1029. <http://doi.org/10.1634/stemcells.22-6-1015>
- Zhou, W., Fong, M. Y., Min, Y., Somlo, G., Liu, L., Palomares, M. R., ... Wang, S. E. (2014). Cancer-Secreted miR-105 Destroys Vascular Endothelial Barriers to Promote Metastasis. *Cancer Cell*, *25*(4), 501–515. <http://doi.org/10.1016/j.ccr.2014.03.007>
- Zlotnik, A. (2006). Involvement of Chemokine Receptors in Organ-Specific Metastasis. In *Infection and Inflammation: Impacts on Oncogenesis* (Vol. 13, pp. 191–199). Basel: KARGER. <http://doi.org/10.1159/000092973>
- Zlotnik, A., & Yoshie, O. (2000). Chemokines : A New Classification System and Their Role in Immunity, *12*(3), 121–127.